THE MICROMORPHOLOGY OF YOUNGER DRYAS-AGED BLACK MATS FROM NEVADA, ARIZONA, TEXAS AND NEW MEXICO

by

Erin Harris-Parks

A Prepublication Manuscript Submitted to the Faculty of the

DEPARTMENT OF GEOSCIENCES

In Partial Fulfillment of the Requirements
for the Degree of

MASTER OF SCIENCE

In the Graduate College
THE UNIVERSITY OF ARIZONA
2014

Abstract

Black mats are organic-rich sediments and soils that form in wet environments associated with spring discharge. A micromorphological and geochemical analysis of 25 Younger Dryas-aged (12.9-11.6 ka BP) and younger, black mats was conducted to determine their composition and depositional environment. Samples were collected from previously documented and radiocarbon-dated sites in Arizona, New Mexico, Texas and Nevada. Geochemically, black mats are highly variable and can range from 0-51.0% $CaCO_3$ and 0.4-21.8% organic matter. Micromorphological analyses were conducted on thin sections using polarized and fluorescent light. These analyses determined that black mats contain a variety of organic matter including humic acids, fine (5-20μm) plant fragments, diatoms, phytoliths, and gastropods. The dominant type of organic matter is derived from herbaceous plants, contradicting previous studies that supported algal or charcoal sources. Differences in the micromorphological characteristics of the samples revealed that black mats formed as three different types: organic horizons, moist soils and diatomaceous ponded sediments. The relationship between topography and the water table governs the formation of these different types. Black mat formation peaked in Nevada and Arizona during and directly after the Younger Dryas due to a raised water table which provided optimal conditions for spring discharge and heightened plant productivity.

Keywords: micromorphology, black mats, Younger Dryas, algae, desert, paleoclimate, groundwater, thin sections, fluorescence microscopy

Introduction

Black mats are organic-rich sediment layers and soils preserved in late Pleistocene and early Holocene stratigraphic sequences. They are found throughout central and western North America and even in the Atacama Desert in northern Chile (Quade et al., 1998; Haynes, 2008; Pigati et al., 2009; Pigati et al., 2012). The term black mat has been applied to a wide variety of soil and sediment types including Mollisols, Aqolls, algal mats, diatomites and marls (Haynes, 2008). Previous studies established that black mats form in wet environments associated with spring discharge and elevated water tables (Quade et al., 1998; Haynes, 2008; Pigati et al., 2009). Because black mat formation is so closely related to moist conditions, their presence in present day arid to semi-arid environments suggests that they formed under different environmental conditions compared to today.

Previous studies have documented dramatic increases in black mat formation associated with the start of the Younger Dryas (YD) climatic event. Quade et al. (1998) determined that black mat formation in southern Nevada peaked from 11,200-10,000 ^{14}C yr BP. Haynes (2008) called black mats the **"**stratigraphic manifestation of the Younger Dryas." after identifying 70 YD-aged black mats associated with archaeological sites in North America. The YD was a brief period that lasted from 11,000-10,000 ^{14}C yr BP (12.9-11.6 ka yrs BP) and marked return to cooler conditions following a general warming trend after the end of the last glacial maximum (Mangerud et al., 1974; Anderson, 1997; Severinghaus et al., 1998). Greenland ice cores provide high-resolution records of colder and dryer conditions in the North Atlantic for the YD. Some records indicate that conditions could have been up to 15±3°C colder than present in the North Atlantic (Severinghaus et al., 1998).

However, most of North America did not experience these glacial-like conditions. Paleoclimate studies in the southwest (SW) indicate moister conditions associated with the YD, including speleothem growth and paleolake expansion (Broughton et al., 2000; Polyak et al., 2004; Briggs et al., 2005). Conversely, other records indicate drying and warming trends in the Midwest during the YD (Holliday et al., 2011; Wang et al., 2012). Additionally, the disappearance of the Clovis culture, the earliest widespread culture to occupy all of North America, and the extinction of an estimated 35 genera of large mammals appears to have coincided with the onset of the YD (Haynes, 2008; Polyak et al., 2012). Therefore, the peak in black mat formation and the onset of the YD mark major cultural and biological changes.

Adding to the significance of black mats is the theory that a 12.9 ka extraterrestrial impact caused YD climate changes, megafaunal extinctions and the demise of the Clovis culture (Firestone et al., 2007). Many of the proposed "impact markers" found in black mats have since been discredited by others citing misidentification, presence in younger black mats, or non-reproducibility (Pinter et al., 2011; Pigati et al., 2012). Firestone et al. (2007) also reported elevated levels of charcoal, soot and carbon spherules in black mats due to widespread wildfires caused by the impact.

Because of the debate surrounding environmental changes during the YD, and the resulting widespread development of black mats, it is important to know the organic and mineral composition of black mats in order to better understand how they formed. Previous studies have identified black mats as organic rich, silty layers (Quade et al., 1998), still others have called them algal mats (Jull et al., 1999; Haynes, 2007b) and finally at Lubbock Lake, the black mat is in fact a white-colored diatomite (Holliday, 1985a; Haynes, 2008). In order to determine their composition, black mat samples from Arizona, Nevada, Texas and New Mexico were collected

and analyzed in thin section and geochemically. Here I present a thorough description of the microscopic and geochemical contents of 25 black mat samples with a strong emphasis on the types and forms of organic matter present. The overall goal of this study is to provide an in-depth understanding of the composition and origins of black mats in order to relate their formation to environmental changes associated with the YD.

Sampling Locations

Murray Springs and the San Pedro Valley, Arizona

The San Pedro Valley is a 240 km long valley, located in the Basin and Range Province of southern Arizona on the border between the Sonoran and Chihuahuan Deserts (Pigati et al., 2009) (Fig. 1). Many of the archaeological sites there contain evidence of Clovis mammoth hunting (Haury, 1953; Haury et al., 1959; Hemmings and Haynes, 1969). In most of these locations, the black mat, referred to as Stratum F_1 or the Clanton Ranch Member, directly overlies the Clovis age strata (Haynes, 2007d). It also formed contemporaneously with Stratum F_{2b}, the Earp Marl (Haynes, 2007c). Radiocarbon dates on the organic matter in the black mat indicate that it formed from 10,800-9,800 ^{14}C yr B.P. (Haynes, 2007a)(Fig. 2).

Murray Springs is an archaeological site in Curry Draw, a tributary of the upper San Pedro Valley. Excavations, which began there in June 1966, uncovered mammoth and bison remains associated with Clovis artifacts, and a Clovis campsite (Haynes, 2007d). The black mat directly overlies the Clovis surface and is described as an organic-rich, silty, smectitic clay with fine angular blocky structure (Haynes, 2007c). Combined pyrolosis and thin layer chromatography analysis of black mat samples from Murray Springs led Haynes (2007b) to conclude that the organic matter was primarily composed of algae.

For this study, micromorphology and bulk samples were collected from Trench 22, Area 4, and Profile B at Murray Springs. Four samples were collected from black mat outcrops along a 35 km stretch of the upper San Pedro Valley. The basal contact of the black mat was included in all of these samples. Four additional samples from the San Pedro Valley were provided by Jesse Ballenger (Statistical Research Inc.).

Lubbock Lake, Texas

Lubbock Lake is located in Yellowhouse Draw, a tributary of the Brazos River, on the Southern High Plains of northwestern Texas (Fig. 1). Lubbock Lake is a well-stratified archaeological site, discovered in 1936, that contains evidence of continuous occupation by Native American populations for the past 11,000 ^{14}C years (Holliday, 1985a). The Paleoindian-aged archaeological deposits are associated with alluvial, spring, marsh, and lacustrine sediments, and include Rancholabrean faunal remains with evidence of butchering (Stafford, 1981; Holliday, 1985a).

The black mat at Lubbock Lake is found in stratum 2A and is described as interbedded laminations of pure diatomite, sapropelic silt, clay, and, phytoliths that contains multiple bison kills associated with Folsom artifacts (Stafford, 1981; Johnson and Holliday, 1981; Holliday, 1985a; Johnson, 1987). The lithologic variability is interpreted to reflect alternating periods of standing water and marsh sediments (Holliday, 1985a). Radiocarbon dates on stratum 2A show that it formed from ~11,000 to 10,000 ^{14}C yrs BP (Holliday, 1985a; Haas et al., 1986) (Fig. 2). For this study, a bock of sediment of the black mat including its overlying and underlying contacts was collected from stratum 2A at Trench 65.

Blackwater Draw, New Mexico

The Blackwater Draw Locality No. 1 archaeological site is located on the Southern High Plains of northeast New Mexico in a basin that flows into Blackwater Draw proper, another tributary of the Brazos River (Fig. 1). Archaeological excavations at the site uncovered Clovis, Folsom, Agate Basin and Cody cultural artifacts, butchered animals and campsites (Haynes, 1995). It is also the site of the proposed oldest prehistoric well in North America, said to have been dug by Clovis people ~11,500 ^{14}C yrs B.C. (Haynes, 1999).

The black mat at Blackwater Draw spans units D and E. According to Haynes (1995), unit D is a lacustrine diatomite interbedded with eolian sands that contains Folsom artifacts and bison bones. Unit E is composed of banded organic diatomaceous silt and sands that formed in a marshy environment. The black mat formed from 10,800-9,800 ^{14}C yrs B.P. (Haynes, 1995)(Fig. 2). One micromorphology sample encompassing both units D and E and the lower contact with unit C was collected. Additionally, one bulk sediment sample was collected.

Southern Nevada springs

The black mat samples from Nevada were collected from sites in the southern Great Basin near Las Vegas (Fig. 1). Black mats form in unit E2 in this region and are characterized by 0.5-4% organic matter, are light to dark grey colored, 20-50cm thick, lack bedding, and are dominated by silt (Quade, 1986; Quade et al., 1998). Stable carbon isotopic values indicate that the organic content of most black mats are very low, which is typical of C_3 plants such as trees, shrubs, grasses and sedges (Quade et al., 1998). Black mat formation is documented from 11,800 to ~7200 ^{14}C yrs BP, with a peak in formation from 10,500-9500 ^{14}Cyrs BP (Quade et al., 1998). Analysis of the faunal remains in these black mats indicates that they formed in localized spring, marsh, and wet soil microenvironments associated with spring discharge (Narvaez, 1995; Quade et al., 1995; Quade et al., 1998). The black mat at Gilcrease Ranch in Las Vegas Valley, Unit II,

is described as a structureless organic-rich silt with mollusks, snails and carbonized plant remains that follows the paleotopography of the spring. It was radiocarbon dated to 10,560±100 and 9920±90 ^{14}C yrs BP (Narvaez, 1995).

A total of eleven different black mats were sampled from this region. Black mat samples with intact structure, collected and studied by Quade et al. (1995), Quade et al. (1998) and Narvaez (1995) were thin sectioned. Original orientation was not preserved. Five of these samples were too small to be thin sectioned and only bulk analyses were performed on them.

Methods

Micromorphology

Micromorphology samples must be collected as undisturbed sediment blocks in order to preserve their original structural characteristics. Rarely, large intact peds could be pulled from the wall and wrapped in toilet paper and packing tape. When the sediments were too friable to be collected in this manner, plaster wraps or electrical junction boxes were used for sampling. For a more detailed description of collection methods see Goldberg and Macphail (2003). Laboratory preparation methods were followed according to Miller and Goldberg (2009). The samples were oven dried at 65ºC for 48 hours. Then, the samples were impregnated using a 7:3 mixture of unpromoted polyester resin and styrene (Advance Coatings, Westminster, MA). Additionally, 5 ml of methyl ethyl ketone peroxide was added to every liter of the mixture as a hardening agent. The samples were left in a fume hood for seven days to allow the resin to absorb into the samples through capillary action. Finally, the impregnated blocks were oven dried at 65ºC for 48 hours. The samples were sent to Quality Thin Sections (Tucson, AZ) and cut into oversize (51x76cm) thin sections. An additional 4 standard size (27x46 mm) thin sections, BM1, BM2, BM3, BM6, were provided for this study by J. Ballenger. All thin sections were analyzed using an Olympus

BX51 petrographic microscope equipped with transmitted polarized light and incident fluorescent light. The thin sections were described using the terminology from Stoops (2003). The abundance of the coarse components was determined using standard point counting techniques.

Carbonate content

Bulk samples were collected from all sites except from the locations where J. Ballenger provided thin section samples. The bulk samples were oven dried at 65ºC for 48 hours. The abundance of calcium carbonate in the samples was determined using a Chittick apparatus (Machette, 1986). This method uses the digestion of carbonate via HCl to produce CO_2 gas. The amount of gas produced from a known sample weight is then used to calculate carbonate content.

Organic matter content

The amount of organic carbon in the samples was measured using the Walkley-Black method (Janitzky, 1986). This method uses potassium dichromate and sulfuric acid to oxidize the organic carbon in a sample. After the reaction is complete, the volume of the unused solution is determined using titration with ferrous sulfate. This amount is then used to calculate the abundance of organic carbon. It is assumed that the amount of organic matter is equal to 1.724 times the amount of organic carbon present.

Site chronologies and radiocarbon dates

Black mats with well documented radiocarbon age control were specifically selected for this study in order to better constrain the chronologic relationship between black mat formation and the YD. A total of 63 radiocarbon dates were collected for the 20 sampling locations. An additional 98 dates from all the published radiocarbon dates on black mats from the region (Nevada, Arizona, southern California, Texas and New Mexico) were included for a total of 161

black mat dates (Fig. 9). Only the San Pedro Valley sites lack radiocarbon dates. However, several of these locations overlie Pleistocene megafauna remains, likely making them contemporaneous with the nearby Murray Springs black mats.

Results

Black mat composition identified through micromorphology

The goal of micromorphological analysis is to determine the mineral and organic components, and the spatial distribution of these materials through direct microscopic observations. The following section outlines the different types of mineral and organic materials found in the thin sections.

Coarse minerals

Quartz grains dominate the coarse mineral (>10μm) component of all the samples. The grains are evenly distributed throughout the matrix, except in LL13-1 and CS13-1, where they appear laminated. The most abundant grain size in all samples is silt (5-63μm) and the majority of samples are composed exclusively of well-sorted, very fine sand (63-100μm) to silt-sized quartz grains. Several samples contain much coarser grain sizes, including rounded, gravel-sized (>2mm) quartz grains. Other minerals present in the samples include feldspars and micas which never constitute more than 1% abundance and show no patterning or significant variation among samples.

Micromass and fabric

The "micromass" component of the samples, defined as any material < 5μm, is composed mainly of clays, very fine calcite crystals, humic acids, and, Fe-hydroxides. The majority of the samples have a brown micromass composed of humic acids absorbed by high base-exchange

clays, such as smectite, (Fig. 3f). (Singh, 1956; Taylor and Glick, 1998). Several samples contain tan-colored micromass due to the presence of micrite, or microcryastalline calcite crystals.

B-fabric, or patterns made by interference colors in the micromass, also varies within the samples (Stoops, 2003). The darkest colored samples have undifferentiated b-fabric, likely because the dark humic acid staining masked the interference colors of the clay (Fig. 3f). However, several samples from the San Pedro Valley display a wide variety of very distinct b-fabrics including porostriated, granostriated, monostriated and crossstriated (Fig. 3a-d). Finally the samples with micrite in the micromass display calcitic crystallitic b-fabric (Fig. 3e)

Coarse plant remains

Preserved plant material and plant decay products are present in all of the black mat samples. Large plant fragments (>200 μm) with visible cell structure are absent in most of the samples. Instead, the samples contain much smaller fragments, generally 20-50μm, in varying abundances. These fragments are opaque to dark brown, lath shaped to rounded and only occasionally show visible internal cell structure. In some samples these dark, fragmented plant remains are so abundant that the entire groundmass is completely opaque and consists almost entirely of this material. In other samples these small remains are scattered randomly throughout the groundmass with no visible orientation. The Texas and New Mexico samples contain elongate, dark brown plant remains all oriented parallel to the surface.

This material is part of the phytoclast organic matter classification group which is composed of the lignin and cellulose tissue from higher plants (Tyson, 1995). Lignin is highly resistant to decay and will remain in the groundmass long after other plant materials have decayed (Tyson, 1995). The phytoclast group appears dark brown to black and usually has light brown edges in transmitted white light (Fig. 3a). The opaque phytoclast subgroup appears

opaque in thin section (Tyson, 1995) (Fig. 4b). Both of forms are present in the black mat samples and are often indistinguishable since the thickness of the slide and the abundance of organic matter can affect the opacity of the phytoclasts. Conversely, charcoal, which is characterized by black color and very well defined internal cell structure is absent in most samples and very rare in a few (Tyson, 1995; Stolt and Lindbo, 2010).

Phytoliths

Phytoliths, which are amorphous silica bodies produced by plants, are present in many of the black mat samples (Mulholland and Rapp, 1992). Most often the phytoliths are distributed randomly throughout the groundmass and appear to be most concentrated in the areas with the darkest groundmass, presumably in areas with the highest concentration of decomposed plant remains. The phytoliths found in the Lubbock Lake and Blackwater Draw samples are still arranged in their original positions within the plant (Fig. 4c). It is impossible to determine the three dimensional shape of the phytoliths in thin section. However, it appears as though the pooid, rondel, elliptical, and rectangular shape classes from Twiss (1992) are represented in the samples.

Gastropods and diatoms

Gastropod remains, often fragmented and unidentifiable, are present in five of the black mat samples. Based on the elongate conic shape of several complete shells, these specimens likely belong to the genus *Gastrocopta* (Burch, 1962) (Fig. 4d). However, observation in thin section does not allow for species-level identification. Many fragmented shells and one complete ostracod are also present in association with the marl deposits at Murray Springs.

Diatoms are only visible in the Lubbock Lake and Blackwater Draw samples (Fig. 4e). They constitute 8% and 33% of the samples' groundmass, respectively. Genus level

identification of the diatoms was based on a study of diatom species on the High Plains by Winsborough (1995) (Fig. 5). The most common genera represented in the samples are *Epithemia* and *Denticula*.

Bone

Bone is present in three black mat samples. Two samples from Murray Springs contain several very small (50-300µm) rounded bone fragments (Fig. 4f). The sample from Lubbock Lake contains a very large bone (~5cm wide) that appears unbroken. This bone is possibly from a bison, because bison kills are common in stratum 2A at the site (Johnson and Holliday, 1981; Johnson, 1987).

Fluorescence microscopy

Fluorescence microscopy is often used as a compliment to micromophological analysis to aid in the identification of organic materials and minerals that appear opaque in transmitted light (Macphail et al., 2004; Goldberg et al., 2009; Mentzer, 2011). In particular, the nature of organic matter under fluorescent light is indicative of characteristics such as cell type (i.e. parenchyma), material (i.e. lignin) and decomposition state (i.e. humified) (Altetmüller and Van Villet-Lanoe, 1990). The black mat samples were observed under fluorescent light to better identify the types of organic matter present.

Haynes (2007c) described the black mat at Murray Springs as an "algal mat" that formed as an algal bloom on standing water. This conclusion was based on combined pyrolosis and thin layer chromatography conducted in 1968 (Haynes, 2007b). Since these analyses, the black mat is commonly referred to as an algal mat although no other study has ever identified, or attempted to identify algae in a black mat (Jull et al., 1999; Haynes, 2008).

Algal mats are primarily composed of green algae, which are easily identified using fluorescent light, as they emit a bright yellow autofluorescence (Puttmann et al., 1994; Taylor and Glick, 1998). Peat and coal deposits derived from algae are called alginites. These deposits are typified by large colonies of *Botryococcus* algae which have visible radial cell arrangement and branching colony structure (Taylor and Glick, 1998; Ji et al., 2010) (Fig. 6c). Laminated algal deposits, or lamalginites, are composed of algae without recognizable structure (Taylor and Glick, 1998). The algal remains in both lamalginites and alginites have bright yellow to orange fluorescence in fluorescent light. Deposits containing decomposed algae, termed bituminites, are also characterized by bright yellow to orange fluorescence that appears no different from the appearance of well-preserved algae (Gutjahr, 1983; Puttmann et al., 1994; Taylor and Glick, 1998) (Fig. 6d). Conversely, non-fluorescing bituminite is composed of humic acids from terrestrial organic matter (Littke, 1993; Taylor and Glick, 1998).

Observation of the black mat samples under blue fluorescent light revealed that the phytoclasts and dark, organic-rich micromass do not fluoresce (Fig. 6). Only the samples containing diatoms or calcitic micromass displayed a green fluorescence, however, these are easily distinguished from the yellow color and shape of the algal colonies in an algal bloom (Fig. 6e).

Carbonate and organic content

Analyses were conducted to determine the abundance of carbonate and organic matter of 21 black mat samples (Fig. 7, Table 2). Organic matter content ranged from 0.4-21.7%. The majority of samples contained less than 4% organic matter and only one sample contained greater than 15% organic matter. Carbonate content was also highly variable and ranged from 0-51.0%. However, all but two of the samples contained <20% carbonate.

Descriptions of black mat types

Although all the black mat samples have many similarities in terms of mineral type, abundance and organic matter, there are still significant morphological and geochemical differences among the black mats sampled in this study. These characteristics appear to group into three major types which were differentiated based on characteristics that provide insight into depositional environments (Table 1).

Type I contains 9.9-21.7% organic matter and 0.5-12.9% carbonate. This type is distinguished by angular blocky structure that often grades into fine laminations. The micromass is composed almost entirely of finely fragmented opaque phytoclasts, which are so abundant that the micromass appears completely opaque. In areas of the thin sections <30 μm thick, the organic matter appears reddened along the edges, and sometimes individual cell structures are visible (Fig. 4a). The coarse mineral component is very minor (4-11%) and silt-sized quartz grains appear to be floating in an opaque matrix. Phytoliths are also present in these layers in abundances of up to 2%. Often, these units are deposited on top of, or interlayered with marl deposits.

Type II black mats have a lower organic component that ranges from 0.6-7.0% organic matter. They are characterized by a much larger coarse and fine mineral component and the absence of layering. These samples are divided into two groups which are differentiated by differences in carbonate content, organic matter and micromass.

Type IIa black mats are characterized by a dark brown micromass, complex b-fabrics and an abundant but variable coarse mineral component. Organic matter ranges from 2.5-7.0% and carbonate content ranges from 0-3.9%. Massive and subangular blocky microstructures are most common. Most samples are dominated by silt in 9-11% abundances. Others are poorly sorted

with gravel to silt sized particles in abundances from 19-49%. Cracks, or slickensides with associated monostriated or porostriated b-fabrics are present in most samples. Other b-fabrics including crossstriated and granostriated are also present in these samples. Phytoliths are present (1-5%) in all of the samples.

Type IIb black mats are characterized by light brown to tan colored micromass due to higher carbonate content (2.1-52.0%). Micritic crystals are often visible in the micromass. Well preserved opaque and non-opaqe phytoclasts are present evenly distributed in the groundmass and are generally very finely fragmented. Organic matter content ranges from 0.6-3.3%. These samples are also characterized by the total absence of phytoliths and the presence of gastropod shells in all but one of the samples. The coarse component of the samples is dominated by silt sized quartz grains with abundances of <1-10%.

Type III black mats are markedly different from the previous samples. These samples have light grey colored massive groundmasses, very weakly speckled b-fabrics and distinct layering where phytoclasts appear oriented parallel to the surface. Organic matter and carbonate content is very low and ranges from 0.9-0.4% and 0-1.75% respectively. The coarse component in these samples consists of silt grains (3-13%) with distinctly layered quartz grains. The samples are dominated by phytoliths and diatoms that appear either well mixed or as alternating layers. Often, phytoliths appear associated *in situ* with plant remains.

Discussion

Black mat composition

Opaque to nearly opaque phytoclasts were present in all samples. Dark to opaque organic matter is formed through desiccation and oxidization when organic material is exposed to oxygen at, or very close to the surface. This generally occurs in areas with strong seasonality and

water table fluctuations (Tyson, 1995). The blackening of organic matter can also be caused by waterlogged conditions (Stoops, 2003). Finally, wetting, drying, and, microbial and faunal activity will crack and fragment the organic material into lath shapes and evenly distribute it throughout the groundmass (Stolt and Lindbo, 2010).

The presence of repeated wetting and drying cycles during black mat formation is also indicated by the well-developed b-fabrics in the matrix (Fig. 3a-d). Microshearing from shrink-swell processes will cause the clay particles to align in the micromass (Kovda and Mermut, 2010). Vertic features such as these are found in many of the samples from the San Pedro valley that are rich in clay.

The absence of large bark and leaf fragments and the abundance of very fine phytoclasts suggests that the original plant material was derived from small herbaceous plants. Herbaceous plants, including grasses, contain 3-10% lignin, which is the decay-resistant material that forms phytolcasts (Tyson, 1995). The other components of herbaceous plants quickly decay into humic acids which bind to the clay particles giving some black mat samples their dark color (Singh, 1956). The abundance of phytoliths in many of the samples also suggest an organic matter source primarily derived from grasses (Mulholland and Rapp, 1992). Most pooid-type phytoliths, which are common in the black mat samples, are produced in leaf epidermis of C_3 grasses (Twiss, 1992). This supports the isotopic data from Quade (1998) which attributed low $\delta^{13}C$ value (-22 to -27‰) of black mats to the presence of decomposed C_3 plants. The major organic input in the black mats is likely from grasses, or other herbaceous phytolith-rich plants. Finally, the absence of ash and near-complete absence of charcoal in all of the samples does not support the theory that the black mats formed by regionally extensive fires caused by an extraterrestrial impact.

Fluorescence

Previous chemical and fluorescence studies on algal deposits show that algae will fluoresce in both preserved and highly decomposed states (Taylor and Glick, 1998). Modern evidence suggests that coalesced algal mats are resistant to oxidization and will be preserved even under subaerial exposure (Teichmüller 1982, Dubreuil et al., 1989). Others report that algae will decay quickly but the gross outline of the colonies will still be visible (DeDeckker, 1988; Dubreuil et al., 1989). Therefore, the lack of fluorescence, or other morphological indicators of algae in black mats indicates that they did not form primarily from large colonial algal blooms. Previous studies have demonstrated that humic rich sediments do not preserve algae (Tayor et al., 1998). Therefore, it is possible that low abundances of algae were once present in the black mats, and have been completely destroyed by the abundant humic acids.

The abundance of non-fluorescing organic material with visible cell structure indicate that black mats did not form as simply from seasonal algal blooms but are instead dominated by the input of organic material from herbaceous plants. The opaque nature of the organic matter present in the black mats appears most similar to the degradofusinite maceral type found in coals. Degradofusinites formed in conditions of desiccation and oxidization, causing their characteristic non-fluorescing, poorly preserved appearance (Taylor and Glick, 1998; Goncalves et al., 2013).

Paleoenvionmental interpretation of black mat types

Type 1 Periodically Saturated Organic Horizons

In order for these organic-rich horizons to form, the production rate of organic materials exceeded the rate of decomposition. The detrital humic plant material (<100μm) in these black mats is very similar to those found in reed, sedge and grass marshes which are characterized by low lignin content and highly decomposed organic matter (Cohen and Spackman, 1977; Taylor

and Glick, 1998). These types of deposits generally form in environments with high water tables dominated by herbaceous plants (Taylor and Glick, 1998). Bouma et al. (1990) determined that saturated soils are characterized by layering, massive structure, and abundant diatoms. Although layering and massive structure are present in these samples, the absence of diatoms and the highly fragmented state of the organic matter suggests that these black mats did not form in permanent standing water conditions.

The characteristic black color of the organic matter in these layers results from decomposition in oxic conditions and/or microbial attack (Taylor and Glick, 1998). These layers could be oxidized in two ways: 1) Groundwater has high oxidizing capacity. Studies show that aquifer groundwater in Nevada and Arizona contains high amounts of dissolved oxygen (Winograd and Robertson, 1982). 2) The desiccation of peat due to periodic drying will promote decomposition or ripening. This allows for plant decomposition through oxidization, faunal activity and humification resulting the formation of secondary humus peats (Babel, 1975; Bouma et al., 1990). Alternating wet and dry periods during peat formation will create blackened plant fragments and angular blocky structure both of which are present in the black mat samples (Taylor and Glick, 1998; Stolt and Linbo, 2010).

The absence of diatoms, which are characteristic of prolonged permanently saturated peats, also suggests that these samples experienced periodic desiccation (Bouma et al., 1990). Silica can dissolve based on changes in pH, temperature and salinity (Ryves et al., 2006). The absence of diatoms in these samples is due to either unfavorable living conditions from periodic wetting and drying, or dissolution caused by changes in pH during periods of desiccation. Corroded phytoliths in these thin sections also suggests silica dissolution is occurring.

All of the samples in this category were deposited very close to spring vents (Narvaez, 1995, Haynes, 2007c). This setting provides a readily available source of water capable of sustaining at least seasonal periods of standing water creating highly productive plant communities. Peat is defined by Tarnocai and Schuppli (1987) as having >17% organic carbon (>29% organic matter). None of the type I black mats contain enough organic matter to be considered peat possibly because of decomposition from frequent desiccation, or that they formed over too brief a period to accumulate sufficient amount of organic matter. Regardless, given their similarity to herbaceous peat deposits, type I black mats, which formed almost exclusively at Murray Springs, Arizona, formed in peat-like conditions in which organic matter accumulated in water saturated conditions with layering and low mineral input. Periodic, possibly seasonal drying of these deposits caused the organic matter to decompose through oxidization, and bacterial decay. This caused the organic material to appear blackened through humification and fragment due to desiccation and breakdown. The corroded appearance of the phytoliths suggest that these conditions likely caused silica dissolution, explaining the absence of diatoms, which are usually characteristic of saturated sediments.

Type II Moist Soils

This type is characterized by a well-mixed groundmass and a much higher coarse mineral component. The absence of bedding, and the even distribution of organic material and coarse sized minerals in this type of black mat indicate that they formed in unsaturated, heavily bioturbated conditions. Based on their micromorphological and geochemical characteristics this type was subdivided into two groups with many samples showing intermediate characteristics between the two. The major difference between the two groups is carbonate content, which is determined by parent material, rather than differences in depositional environment.

Type IIa black mats are almost exclusively located in Arizona, and are characterized by dark brown micromasses and vertic properties such as complex b-fabrics, slickenslides, rounded clay and calcite anorthic clasts, and blocky structure. These are indicative of cyclic shrinking and swelling of clays. These shrink-swell associated b-fabrics require 550 or more years to develop indicating that these samples experienced prolonged exposure to these conditions in order to form (Paranjape et al., 1997).

Mixing from bioturbation injects oxygen into the subsurface stimulating decomposition of plant material, and the rapid humification of grasses (Taylor and Glick, 1998). This will produce humic acids which bind to the smectite clays present in the San Pedro Valley giving these samples their dark appearance.

The coarse mineral content of this type varies from well-sorted silt to poorly sorted coarse sand-sized grains. In the coarser samples, the grain size and abundance does not change between the black mat and the lower unit. This suggests that gravelly channels stabilized during this period allowing plant productivity and soil forming processes to occur for a number of years.

Type IIb black mats, are largely dominated by the Nevada samples, but also include several Arizona samples. The limestone-dominated mountains surrounding the Nevada black mats contribute to the high carbonate contents found in this type. Type II black mats are characterized by have lighter micromasses due to the increased abundance of carbonate, and decreased amounts of organic matter. Humic acid staining is absent because $CaCO_3$ inhibits the sorption of humic acids, allowing them to be leached from these sediments (Singh, 1956). Additionally, the presence of carbonate in sediments will reduce acidity of system, thus promoting more rapid decay of plant materials, especially in aerobic conditions. (Taylor and

Glick, 1998). Therefore, the only visible organic matter present in these samples are lath shaped phytoclasts, which have been evenly distributed throughout the sediments from bioturbation.

$CaCO_3$ also restricts the shrink swell capacity of soils, and can mask the appearance of b-fabrics, explaining why complex b-fabrics are absent in these samples (Pal et al., 2001; Kovda and Mermut, 2010). The abundance of iron impregnations, nodules and hypocoatings in these samples do however indicate that these samples formed in wet conditions.

Type II soils formed in well-aerated moist sediments. The presence of shrink swell features and iron staining indicates that these soils experienced moist conditions that promoted elevated levels of plant growth. The decomposed nature of the organic matter in these types is due to biological and chemical decay processes that were able to continue, uninhibited by saturated or anoxic conditions. This type of black mat formed as a moist soil likely close to areas of spring discharge. They were located at slightly higher elevations, or in areas with a lower water table than type I black mats and did not experience standing water. Instead, moist, intensely bioturbated soils formed due to their proximity to the shallow water table below or through slow lateral saturation due to spring seepage.

Type III Diatomaceous Ponded Sediments

The type III black mats from Lubbock Lake and Blackwater Draw have characteristics quite distinct from the other black mats. Microlamintations of silt, phytoliths, organic matter, and diatoms indicate that these deposits formed in very low energy, standing water environments. Saturated conditions persisted throughout their formation as evidenced by the lack of bioturbation and the massive structure that lacks micromorphological evidence for desiccation. The low organic matter content can be explained by oxidization from well oxygenated ground

waters or formation in a shallow lacustrine environment that lacked significant plant colonization.

The identification of diatoms in these thin sections is supported by the findings of Winsborough (1995). At Lubbock Lake the very high abundance of *E. argus*, *D. elegans* and *R. gibberula* at ~10,000 yrs BP are interpreted as a shallow muddy ponded environment, reflecting a decrease in water level at this time (Holliday, 1995). At Blackwater Draw, the diatom assemblage is dominated by *R. gibba*, and *E. adnanta* from ~10700-10200 and is interpreted as a shallow pond or marsh with mud or vegetation with an estimated water depth of ≤1 meter (Winsborough, 1995). These interpretations support the micromorphological interpretations and indicate that these samples formed in shallow, lacustrine to marsh-like conditions of permanent, low energy standing water. Diatoms are considered a hard-bodied form of algae. Therefore, the white colored "black mats" on the High Plains are the only black mats to have a significant algal component.

Facies model and regional water table inferences

The presence of black mats in arid and semi-arid regions with features related to water presence or saturation indicate that they all formed in wet conditions. The three main types of black mats identified can be related to interactions with local/regional topography and the water table (Fig. 8).

The characteristics identified in type I, IIa, and IIb black mats describe the best example of these types. In reality, several black mats can be seen grading from type I to IIa to IIb. These types represent a continuum where either lateral or temporal changes in organic matter productivity and mineral input can change these black mats from one type to another. Type I black mats form in periodically saturated swamp-like environments where plant productivity is

very high and mineral input is very low. This type of black mat can slowly grade into type IIa, which forms in wet soils with slightly lower plant productivity where bioturbation causes significant mixing with the underlying sediments. As carbonate content increases, due to limestone rich parent material, type IIa grades to type IIb.

Because all of these types occur in black mats from both Arizona and Nevada, it suggests that the appearance of black mats is heavily dictated by the topographic relation to the water table and to a lesser degree geographic location. The final type of black mat occurs, with great similarity in two samples from the High Plains. These samples have evidence for permanent standing shallow water. It is clear that these black mats formed in a system separate from type, I and II, which lack evidence for permanent standing water conditions. The morphological distinctions between these types suggests regional differences in effective moisture between the High Plains and the SW deserts, which are most likely controlled by differences in larger climatic systems.

Timing of black mat formation

Black mats are not unique to the YD. They formed in the Atacama Desert in Chile as long as 40 thousand years ago while others formed in southern Nevada ~500ys ago (Quade et al., 1998; Pigati et al., 2012). The micromorphological and geochemical characteristics of YD-aged and 7,200 ^{14}Cyr-aged black mat samples in Nevada are indistinguishable, indicating that they formed under similar environmental conditions. What makes YD-aged black mats unique is their abundance and large geographic distribution (Fig. 9). The widespread emergence of black mats associated with the YD indicates favorable conditions for formation occurred across a larger area than previous or more recent times. The sharp increase in formation right at the onset of the YD suggests that there was not a lag time between the onset of the YD and black mat formation. This

is possible since black mats are composed of herbaceous plants which have a much faster response time to environmental changes than larger plants.

Black mat formation appears most abundant during the latter part of the YD and remains elevated until ~8,500 ^{14}Cyrs B.P. (Fig. 9). Quade et al. (1998) demonstrated that modern contamination is not a significant issue in arid settings. Therefore, it is more likely that the peak in black mat formation from ~10,500-9,500 ^{14}Cyrs BP is due to the lasting effects of regional YD environmental changes that appear to outlive the YD by over 1,000 years.

Other proxies for environmental conditions

Several paleoenvironmental proxies support the prevalence of wetter conditions in the SW during the YD. Studies on speleothem growth in Arizona and New Mexico during the YD determined that cooler moister conditions with increased winter precipitation prevailed during the YD (Wagner et al. 2010; Polyak et al 2004; Asmerom et al., 2010). In one instance the timing of these wetter exceed the YD by over 1,000 years, supporting the black mat radiocarbon ages in suggesting that wetter conditions persisted long after the termination of the YD. Lake expansion also occurred during the YD in Great Basin at Lake Bonneville and Pyramid Lake (Broughton et al., 2000; Briggs et al., 2005).

Paleoclimatic reconstructions from various regions in the Southern High Plains lack a universal response to the YD. Lowland areas shifted from alluvial to lacustrine environments at the onset of the YD while upland areas experienced episodic dune accretion and soil formation (Holliday et al., 1996; Holliday et al., 2011). These changes do suggest an overall warming trend and decline in effective moisture that initiated during the YD and intensified during the Early Holocene.

Atmospheric circulation models proposed by Wang et al. (2012), Polyak et al. (2004), and Yu and Wright (2001) explain the seeming disparity between moister conditions in the SW and dryer conditions in the High Plains. When the Northern hemisphere cools as it did during the YD and the Heinrich 1, the Intertropical Convergence Zone (ITCZ) and Polar Jet Stream shift south (Polyak et al., 2004; Wang et al., 2012). Consequently, storm tracks shift south leading to wetter conditions in the southwestern US (Wang et al., 2012). Yu and Wright (2001) hypothesized that arctic air was trapped by the Laurentide ice sheet during the YD, allowing warm air from the Caribbean to penetrate into the continental interior, explaining a warming trend in the High Plains.

Conclusions

Micromorphological analysis of 25 black mat samples indicate that all black mats contain a variety of organic matter forms including humic acids, lignin rich plant fragments, gastropods, phytoliths and diatoms. Contrary to previous studies, fluorescing algal colonies and charcoal are effectively absent in all of the samples, indicating that black mats did not form as algal blooms or from meteorite impact fires. Instead, black mats formed through the high input of herbaceous or grassy plants, which grew in stable, moist settings. Miromorphological and geochemical analysis of the samples showed that black mats characteristics group into three main types. Black mats from Arizona and Nevada range from peat-like deposits to moist soils depending on their topographic position relative to the water table. Their formation peaked in association with the YD due to a raised water table and greater effective moisture. Conversely, black mats from the High Plains formed as lower effective moisture lowered the water table and created shallow ponded sediments. The differences in these systems are related to broader atmospheric circulation changes caused by the YD. However the persistence of black mat formation beyond

the end of the YD suggests a lag between the termination of the YD and the localized changes it incurred. As for the suggestions that bolide-induced climate changes affected human populations and caused catastrophic fires across North America, black mats can no longer be used in that argument. These sediments represent naturally occurring organic-rich deposits that formed in response to changes in effective moisture, in a similar fashion both before, during and after the YD.

Acknowledgements

This work was funded by the Paul S. Martin Scholarship and the Argonaut Archaeological Research fund. I would like to thank Jesse Ballenger, Rachel Cajigas, Jennifer Kielhofer, Amy Schott and Vance Holliday for providing field and laboratory assistance. Finally, I would like to thank Paul Goldberg, Chris Miller, Susan Mentzer and David Killick for guidance in thin section interpretation and access to microscopic equipment.

Works cited

Altemüller, H.J., Van Villet-Lanoe, B., 1990. Soil thin section fluorescence microscopy. In: Douglass, L.A., (Ed.), Developments in Soil Science Volume 19. Elsevier, pp. 565-579.

Anderson, D.E., 1997. Younger Dryas research and its implications for understanding abrupt climatic change. Progress in Physical Geography 21 (2), 230-249.

Asmerom, Y., Polyak, V.J., and Burns, S.J., 2010. Variable winter moisture in the Southwestern United States linked to rapid glacial climate shifts. Nature Geoscience 3, 114-117.

Babel, U., 1975. Micromorphology of soil organic matter. In: Gieseking, J. E., (Ed.), Soil Components. Springer-Verlag, New York, pp. 369-473.

Bouma, J., Fox, C.A., Miedema, R., 1990. Micromorphology of hydromorphic soils: applications for soil genesis and land evaluation. In: Douglass, L.A. (Ed.) Soil Micromorphology: A Basic and Applied Science. Amsterdam, New York, Elsevier, pp. 257-278.

Briggs, R. W., Wesnousky, S. G., and Adams, K. D., 2005. Late Pleistocene and late Holocene lake highstands in the Pyramid Lake subbasin of Lake Lahontan, Nevada, USA. Quaternary Research, 64 (2), 257-263.

Broughton, J. M., Madsen, D. B., and Quade, J., 2000. Fish remains from Homestead Cave and lake levels of the past 13,000 years in the Bonneville basin. Quaternary Research 53 (3), 392-401.

Burch, J. B., 1962. How to know the eastern land snails; pictured-keys for determining the land snails of the United States occurring east of the Rocky Mountain Divide. Dubuque, Iowa, W.C. Brown Co.

Cohen, A. D., and Spackman, W., 1980. Phytogenic organic sediments and sedimentary environments in the Everglades mangrove complex of Florida USA 3. The alteration of plant material in peats and the origin of coal macerals: Palaeontographica Abteilung B Palaeophytologie 172 (5-6), 125-149.

De Deckker, P., 1988. Large Australian lakes during the last 20 million years: sites for petroleum source rock or metal ore deposition, or both? In: Fleet, A.J., Kelts, K., Talbot, M.R., (Eds), Lacustrine Petroleum Source Rocks. Geological Society of London Special Publication 40, pp. 45-58

Dubreuil, C., Derenne, S., Largeau, C., Berkaloff, C., Rousseau, B.R., 1989. Mechanism of formation and chemical structure of Coorongite-1. Role of the resistant biopolymer and of the hyrdocarbons of B*otryococcus braunii.* Ultrastructure of Coorongite and its relationship with Torbanite. Organic Geochemistry 14, 543-553.

Firestone, R. B., et al., 2007. Evidence for an extraterrestrial impact 12,900 years ago that contributed to the megafaunal extinctions and the Younger Dryas cooling. Proceedings of the National Academy of Sciences of the United States of America 104 (41), 16016-16021.

Miller, C.E., Goldberg, P., 2009. Micromorphology and Paleoenvironments Larson. In: M.L., M. Kornfeld, and G.C. Frison (Eds.), Hell Gap: Stratified Paleoindian Campsite at the Edge of the Rockies. University of Utah Press, Salt Lake City, pp. 72-89.

Goldberg, P., and Macphail, R. I., 2003. Short contribution: Strategies and techniques in collecting micromorphology samples. Geoarchaeology-an International Journal 18 (5), 571-578.

Goncalves, P. A., Mendonca, J. G., Mendonca, J. O., da Silva, T. F., and Flores, D., 2013. Paleoenvironmental characterization of a Jurassic sequence on the Bombarral sub-basin

(Lusitanian basin, Portugal): Insights from palynofacies and organic geochemistry. International Journal of Coal Geology 113, 27-40.
Gutjahr, C.C.M.,1983. Introduction to incident-light microscopy of oil and gas source rocks: Geol. En Mijnbouw 62, 417-425.
Haas, H., Holliday, V., and Stuckenrath, R., 1986. Dating of Holocene stratigraphy with soluble and insoluble organic fraction at the Lubbock Lake archaeological site, Texas - an ideal case-study. Radiocarbon 28 (2A), 473-485.
Hatte, C., Hodgins, G., Holliday, V.T., Jull, A.J.T., 2010. Dating human occupation on diatom-phytolith-rich sediment: case studies of Mustang Spring and Lubbock Lake, Texas, USA. Radiocarbon 52, 13-24.
Haury, E.W., Antevs, E., Lance, J.F., 1953. Artifacts with mammoth remains, Naco, Arizona. American Antiquity 23 (1), 2-27.
Haury, E.W., Sayles, E.B., Wasley, W.W., 1959. The Lehner mammoth site, southeastern Arizona. American Antiquity 25, 2–30.
Haynes, C.V, 1995. Geochronology of paleoenvironmental change, Clovis type site, Blackwater Draw, New Mexico. Geoarchaeology 10 (5), 317-388.
Haynes, C.V., Stanford, D.J., Jodry, M., Dickenson, J., Montgomery, JL., Shelly, P.H., Rovner, I., Agogino, G.A., 1999. A Clovis well at the type site 11,500 B.C.: The oldest prehistoric well in America. Geoarchaeology 14 (5), 455-470.
Haynes, C.V., 2007a. Appendix A: Radiocarbon dating at Murray Springs and Curry Draw. In: Haynes Jr., C.V., Huckell, B.B. (Eds.), Murray Springs: a Clovis Site with Multiple Activity Areas in the San Pedro Valley, Arizona. The University of Arizona Press, Tucson, pp. 229–239.
Haynes, C.V., 2007b, Appendix B: nature and origin of the black mat, stratum F2. In: Haynes Jr., C.V., Huckell, B.B. (Eds.), Murray Springs: a Clovis Site with Multiple Activity Areas in the San Pedro Valley, Arizona. The University of Arizona Press, Tucson, pp. 240–249.
Haynes, C.V., 2007c, Quaternary geology of the Murray Springs Clovis site. In: Haynes Jr., C.V., Huckell, B.B. (Eds.), Murray Springs: a Clovis Site with Multiple Activity Areas in the San Pedro Valley, Arizona. The University of Arizona Press, Tucson, pp. 16–56.
Haynes, C.V., 2007d, Clovis investigations in the San Pedro Valley, In: Haynes Jr., C.V., Huckell, B.B. (Eds.), Murray Springs: a Clovis Site with Multiple Activity Areas in the San Pedro Valley, Arizona. The University of Arizona Press, Tucson, pp. 1-15.
Haynes, C.V., Jr., 2008. Younger Dryas "black mats" and the Rancholabrean termination in North America. Proceedings of the National Academy of Sciences of the United States of America 105(18), 6520-6525.
Hemmings, E.T., Haynes Jr., C.V., 1969. The Escapule mammoth and associated projectile points, San Pedro Valley, Arizona. Journal of the Arizona Academy of Science 5, 184–188.
Holliday, V. T., 1985a. Archaeological geology of the Lubbock Lake site, southern High-Plains of Texas. Geological Society of America Bulletin 96 (12), 1483-1492.
Holliday, V. T., 1985b. Early and middle Holocene soils at the Lubbock Lake archeological site, Texas. Catena 12 (1), 61-78.
Holliday, V. T., 1995. Stratigraphy and paleoenvironments of Late Quaternary valley fills on the Southern High Plains. Boulder, Colorado, Geological Society of America.
Holliday, V. T., Meltzer, D. J., and Mandel, R., 2011. Stratigraphy of the Younger Dryas Chronozone and paleoenvironmental implications: Central and Southern Great Plains. Quaternary International 242 (2), 520-533.

Huckleberry, G., Beck, C., Jones, G. T., Holmes, A., Cannon, M., Livingston, S., and Broughton, J. M., 2001. Terminal Pleistocene/early Holocene environmental change at the sunshine locality, north-central Nevada, USA. Quaternary Research 55 (3), 303-312.

Janitzky, P.,1986. Organic Carbon (Walkley-Black Method). In: M.J. Singer and P. Janitsky, (Eds.), Field and Laboratory Procedures Used in a Soil Chronosequence Study. USGS Bulletin 1648, United States Government Printing Office, Washington D.C., pp. 34-36.

Ji, L., Yan, K., Meng, F., and Zhao, M., 2010. The oleaginous Botryococcus from the Triassic Yanchang Formation in Ordos Basin, Northwestern China: Morphology and its paleoenvironmental significance. Journal of Asian Earth Sciences 38 (5), 175-185.

Johnson, E., and Holliday, V. T., 1981. Late Paleo-Indian activity at the Lubbock Lake site Texas USA. Plains Anthropologist 26 (93), 173-193.

Jull, A.J.T., Haynes, C.V., Jr., Donahue, D.J., Burr, G.S., & Beck, J.W., 1999. Radiocarbon ages at Murray Springs, Arizona and the influence of climate change on Clovis man. Proceedings of the Third Conference on ^{14}C and Archaeology. Lyon, France, pp. 339-343.

Kovda, I., Mermut, A., 2010. Vertic features. In: Stoops, G., Marcelino, V. & Mees, F. (Eds.), Interpretation of Micromorphological Features of Soils and Regoliths. Elsevier, Amsterdam, pp. 109–127.

Littke, R., 1993. Deposition, diagenesis and weathering of organic matter-rich sediments. Lecture Notes in Earth Sciences 47, 218.

Machette, M., 1986, Calcium and magnesium carbonates. In: M.J. Singer and P. Janitsky (Eds.), Field and Laboratory Procedures Used in a Soil Chronosequence Study. USGS Bulletin 1648, United States Government Printing Office, Washington D.C., pp. 30-33.

Mangerud, J., Andersen, S. T., Berglund, B. J., and Donner, J. J., 1974. Quaternary stratigraphy of Norden, a proposal for terminology and classification. Boreas 3, 109–128.

Mendonca, J.G., Chagas, R.B.A., Menezes, T.R., Mendonca, J.O., da Silva, F.S., Sabadini-Santos, E., 2010. Organic facies of the Oligocene lacustrine system in the Cenozoic Taubate basin, Southern Brazil. International Journal of Coal Geology 84, 166-178.

Mentzer, S. M., 2011. Macro- and micro-scale geoarchaeology of Üçağizli Caves I and II, Hatay, Turkey. Ph.D Thesis, University of Arizona, Tucson.

Mulholland, S.C., Rapp, G. R., 1992. Phytolith systematics: an introduction. In: Rapp, G. R. Mulholland, S. C., (Eds.), Phytolith Systematics: Emerging Issues. New York, Plenum Press, pp. 1-14.

Narvaez, C. de, 1995. Paleohydology and paleotopography of a Las Vegas Spring. M.S. thesis, Northern Arizona University, Flagstaff.

Pal, D. K., Balpande, S. S., and Srivastava, P., 2001. Polygenetic Vertisols of the Purna Valley of central India. Catena 43(3), 231-249.

Paranjape, M.V., Pal, D.K., Deshpande, S.B., 1997. Genesis of non-vertic deep Black soils in a basaltic landform of Maharashtra. Journal of the Indian Society of Soil Science 45, 174–180.

Pigati, J.S., Bright, J.E., Shanahan, T.M., Mahan, S.A., 2009. Late Pleistocene paleohydrology near the boundary of the Sonoran and Chihuahuan Deserts, southeastern Arizona, USA. Quaternary Science Reviews 28, 286-300.

Pigati, J.S., Miller, D.M., Bright, J.E., Mahan, S.A., Nekola, J.C., Paces, J.B., 2011. Chronology, sedimentology, and microfauna of groundwater discharge deposits in the central Mojave Desert, Valley Wells, California. Geological Society of America Bulletin 123, 2224-2239.

Pigati, J. S., Latorre, C., Rech, J. A., Betancourt, J. L., Martinez, K. E., and Budahn, J. R., 2012. Accumulation of impact markers in desert wetlands and implications for the Younger Dryas impact hypothesis. Proceedings of the National Academy of Sciences of the United States of America109 (19), 7208-7212.

Pinter, N., Scott, A. C., Daulton, T. L., Podoll, A., Koeberl, C., Anderson, R. S., and Ishman, S. E., 2011. The Younger Dryas impact hypothesis: A requiem. Earth-Science Reviews 106 (3-4), 247-264.

Polyak, V.J., Rasmussen, J.B.T., and Asmerom, Y., 2004. Prolonged wet period in the southwestern United States through the Younger Dryas. Geology 32 (1), 5-8.

Polyak, V.J., Asmerom, Y., Burns, S.J., and Lachniet, M.S., 2012. Climatic backdrop to the terminal Pleistocene extinction of North American mammals. Geology 40 (11), 1023-1026.

Puttmann, W., Sun, Y. Z., Kalkreuth, W., 1994. Variation of petrological and geochemical compositions in a sequence of humic coals, cannel coals, and oil shales. Energy & Fuels 8 (6), 1460-1468.

Quade, J., 1986. Late Quaternary environmental-changes in the upper Las-Vegas valley, Nevada. Quaternary Research 26 (3), 340-357.

Quade, J., Pratt, W.L., 1989. Late Wisconsin groundwater discharge environments of the southwestern Indian Springs Valley, southern Nevada. Quaternary Research 31, 351-370.

Quade, J., Mifflin, M. D., Pratt, W. L., McCoy, W., and Burckle, L., 1995. Fossil spring deposits in the southern Great-Basin and their implications for changes in water-table levels near Yucca Mountain, Nevada, during Quaternary time. Geological Society of America Bulletin 107 (2), 213-230.

Quade, J., Forester, R., Pratt, W., and Carter, C., 1998. Black mats, spring-fed streams, and late-glacial-age recharge in the southern Great Basin. Quaternary Research 49 (2), 129-148.

Ryves, D. B., Battarbee, R. W., Juggins, S., Fritz, S. C., and Anderson, N. J., 2006. Physical and chemical predictors of diatom dissolution in freshwater and saline lake sediments in North America and West Greenland: Limnology and Oceanography 51 (3), 1355-1368.

Severinghaus, J.P., Sowers, T., Brook, E.J., Alley, R.B., and Bender, M.L., 1998. Timing of abrupt climate change at the end of the Younger Dryas interval from thermally fractionated gases in polar ice. Nature 391 (6663), 141-146.

Singh, S., 1956. The formation of dark-coloured clay-organic complexes in black soils. Journal of Soil Science 7 (1), 43-58.

Stafford, T., 1981. Alluvial geology and archaeological potential of the Texas Southern High-Plains. American Antiquity 46 (3), 548-565.

Stolt, M.H., Lindbo, D.L., 2010. Soil organic matter. In: Stoops, G., Marcelino, V. & Mees, F. (Eds.), Interpretation of Micromorphological Features of Soils and Regoliths. Elsevier, Amsterdam, pp. 369–396.

Stoops, G. V. M. J., 2003. Guidelines for analysis and description of soil and regolith thin sections. Madison, Wisconson, Soil Science Society of America.

Tarnocai, C., Schuppli, P., 1987. Sedimentary peat in Canadian peatlands. In: Rubec, C., D. A., Overund, R.P., (Eds.) Symposium ’87 Wetlands/Peatlands: proceedings, Edmonton Convention Centre Edmonton, Alberta, Canada, August 23-27, 1987. Wetlands/Peatlands ’87 Coordinator, pp. 25-37.

Taylor, E.L., Taylor, T.N., Collinson, J. W., 1989. Depositional setting and paleootany of Permain and Triassic permineralized peat from the central Tansantarctic Mountains, Antarctica. International Journal of Coal Geology 12, 657-679.

Taylor, G. H.. Glick, D. C., 1998. Organic Petrology: A New Handbook Incorporating Some Revised Parts of Stach's Textbook of Coal Petrology. Berlin, Gebrüder Borntraeger.

Teichmüller, M., 1982. Origin of the petrographic constitents of coal. In: Stach, E., Mackowsky, M.T., Teichmüller, M., Taylor, G.H., Chandra, D., Teichmüller, R., Murchison D.G., Zierke, F, (Eds.), Stach's Textbook of Coal Petrology, 3rd edition. Gerbruder Borntraeger, Berlin, pp. 381-413

Twiss,P., 1992. Predicted world distribution of C_3 and C_4 grass phytoliths, In: Rapp, G. R. Mulholland, S. C., (Eds.), Phytolith Systematics: Emerging Issues. New York, Plenum Press, pp.113-128.

Tyson, R. V., 1995. Sedimentary Organic Matter: Organic Facies and Palynofacies. London, New York, Chapman & Hall.

Wagner, J.D.M., Cole, J.E., Beck, J.W., Patchett, P.J., Henderson, G.M., and Barnett, H.R., 2010. Moisture variability in the southwestern United States linked to abrupt glacial climate change. Nature Geoscience 3, 110-113.

Wang, H., Stumpf, A.J., Miao, X., and Lowell, T.V., 2012. Atmospheric changes in North America during the last deglaciation from dune-wetland records in the Midwestern United States. Quaternary Science Reviews 58, 124-134.

Winograd, I. J., and Robertson, F. N., 1982. Deep oxygenated groundwater - anomaly or common occurrence. Science 216. (4551), 1227-1230.

Winsborough, B. M., 1995. Diatoms. In: Holliday, V.T., (Ed.), Stratigraphy and Paleoenvironments of Late Quaternary Valley Fills on the Southern High Plains, Boulder, Colorado, Geological Society of America pp. 67-84.

Yu, Z. C., and Wright, H. E., 2001. Response of interior North America to abrupt climate oscillations in the North Atlantic region during the last deglaciation. Earth-Science Reviews 52 (4), 333-369.

Figures and Tables

Figure 1. Generalized map of sample locations. Black dots indicate sampling locations. 1) Lubbock Lake. 2) Blackwater Draw. 3) BM 3. 4) Murray Springs, BM6, BM5, SP13-1, SP13-2, SP14-3, SP14-4. 5) Cactus Springs. 6) Corn Creek Flat. 7) Gilcrease Ranch. 8) Browns Spring, Stump Spring. 9) Sandy Valley.

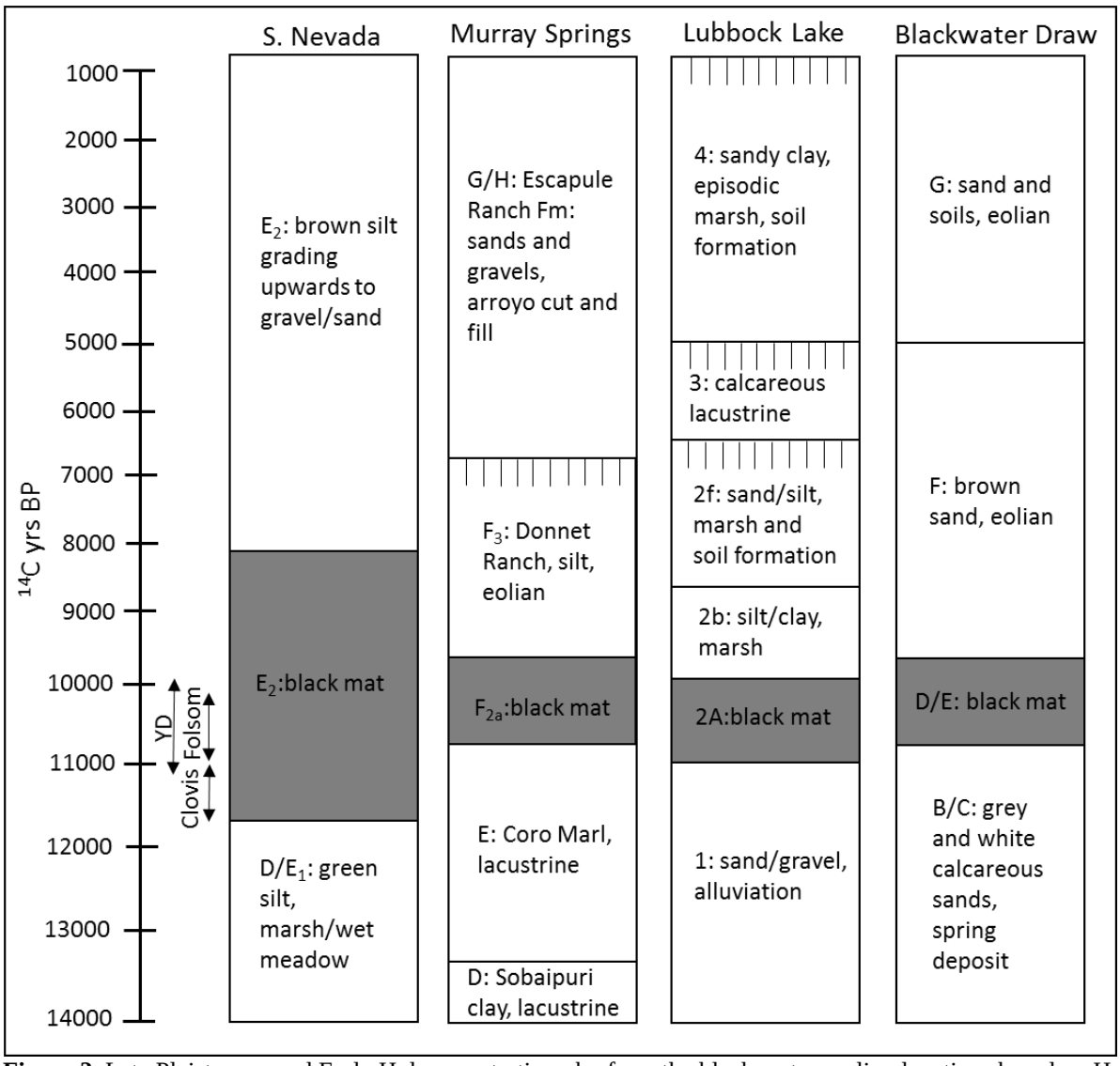

Figure 2. Late Pleistocene and Early Holocene stratigraphy from the black mat sampling locations based on Haynes, 1995; Holliday, 1995; Quade et al., 1995; Quade et al., 1998; Haynes, 2007c.

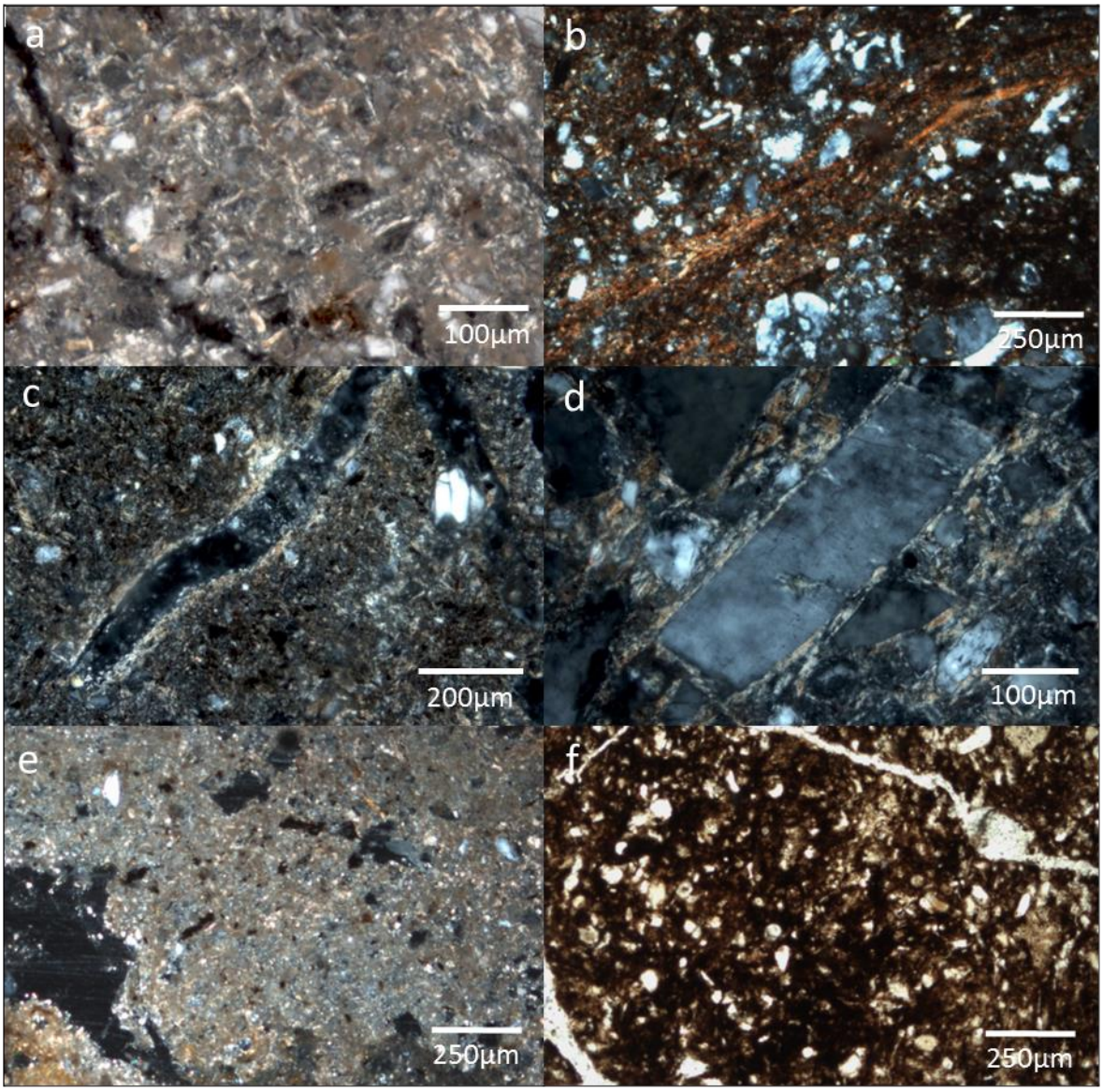

Figure 3. (A) Crossstriated b-fabric, XPL(cross polarized light) in SP13-1. (B) Monostriated b-fabric, XPL in BM2. (C) Porostriated b-fabric, XPL in BM6. (D) Granostriated b-fabric, XPL in BM2 (E) Calcitic crystallitc micromass, XPL in Pah Carb 20. (F) Humic acid-stained micromass PPl (plane polarized light) in BM3.

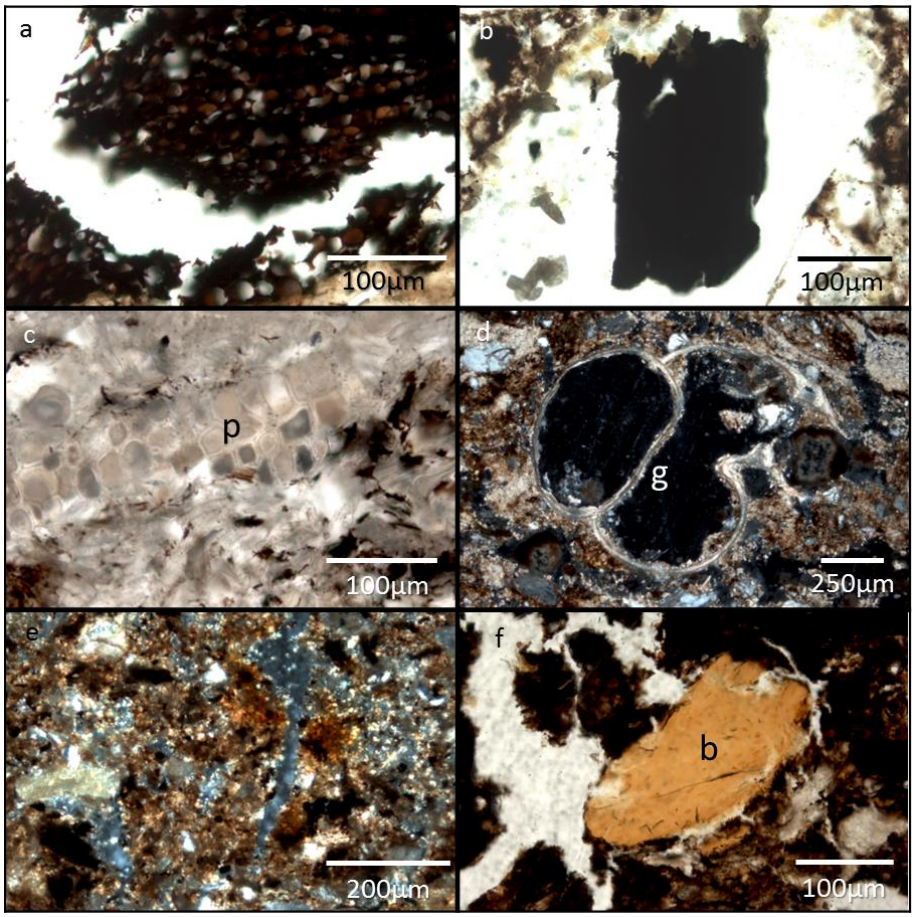

Figure 4. (A) Phytoclast with visible and connected cell structure, PPL in MS13-1a. (B) Opaque phytoclast, PPL in BM1. (C) Aligned rows of phytoliths (p), PPL in LL13-1. (D) Whole gastropod shell (g), XPL in MS13-2B. (E) randomly oriented phytolcasts that appear as opaque black fragments in a calcite rich matrix, PPL in Pah Carb 26. (F) Bone fragment (b), PPL in MS13-2B.

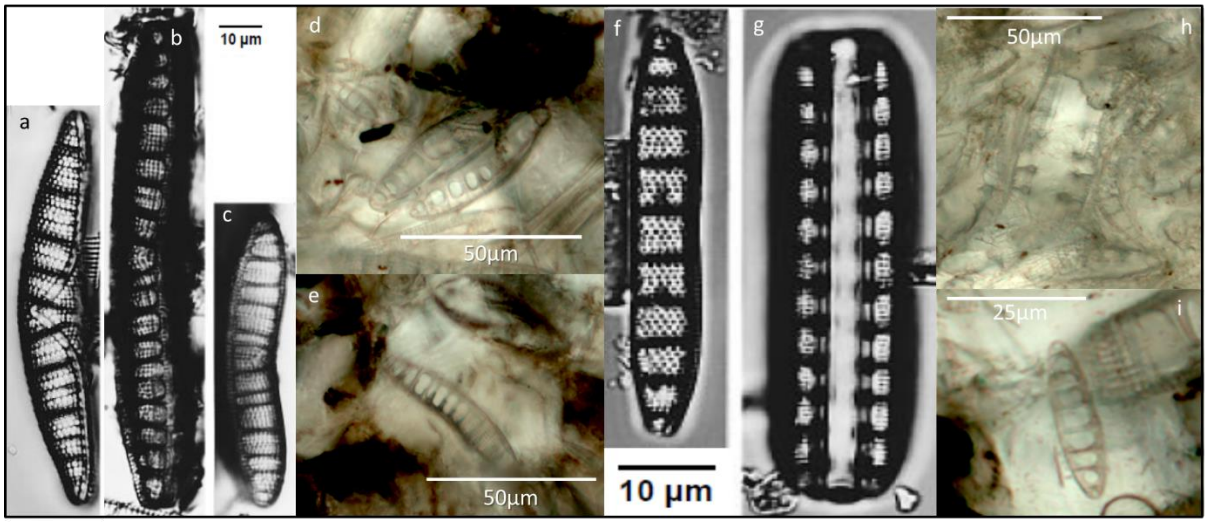

Figure 5. (A) *Epithemia argus*, (B&C) *Epithemia adnata* from Winsborough (1995). (D) A species of *Epithemia* from Lubbock Lake, PPL. (E) A species of *Epithemia* from Blackwater Draw, PPL. (F&G) *Denticula elegans* from Winsborough (1995). (H&I) A species of *Denticula* from Lubbock Lake, PPL.

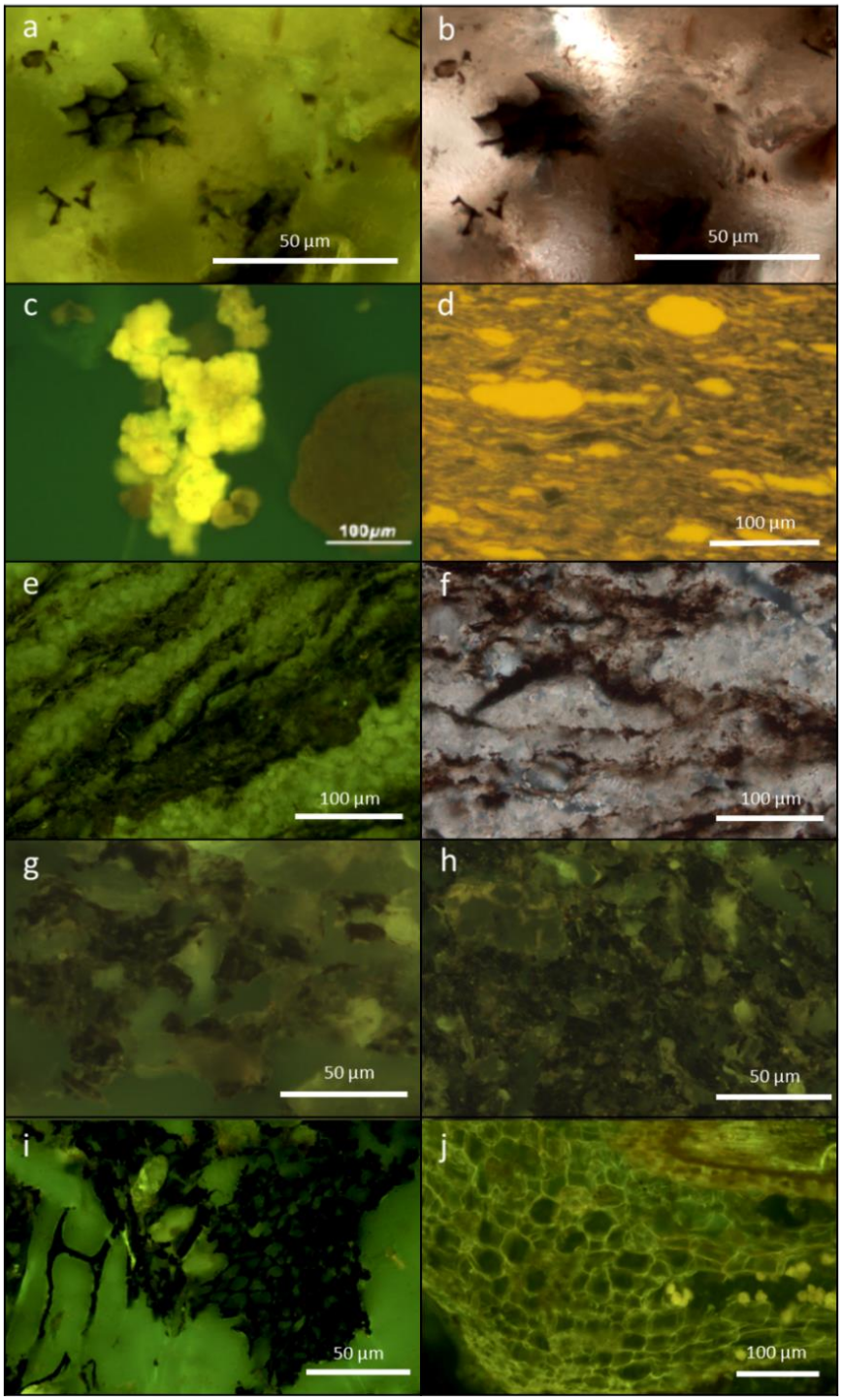

Figure 6. (A) Visible cell structure in blue fluorescent light in Pah Carb 20. (B) The same phytoclast appears opaque in transmitted white light, Pah Carb 20. (C) Well preserved *Botryococcus* colonies from Mendonca et al. (2010), fluorescent light. (D) Filamentous lamalginite with telalgnite (round) in oil shale, blue fluorescent light from Petersen et al. (2006). (E) Layered black mat in green fluorescing marl, blue fluorescent light in MS13-2B. (F) Layered organic matter in marl, PPL in MS13-2B. (G&H) Opaque organic matter lacking fluorescence. The resin has a dull green fluorescence, and the yellow fluorescing objects are phytoliths, blue fluorescent light in MS13-1. (I) Opaque organic matter with cell structure, blue fluorescent light in SVF-87-9. (J) Modern root with bright yellow-green fluorescence, blue fluorescent light in MS13-2B.

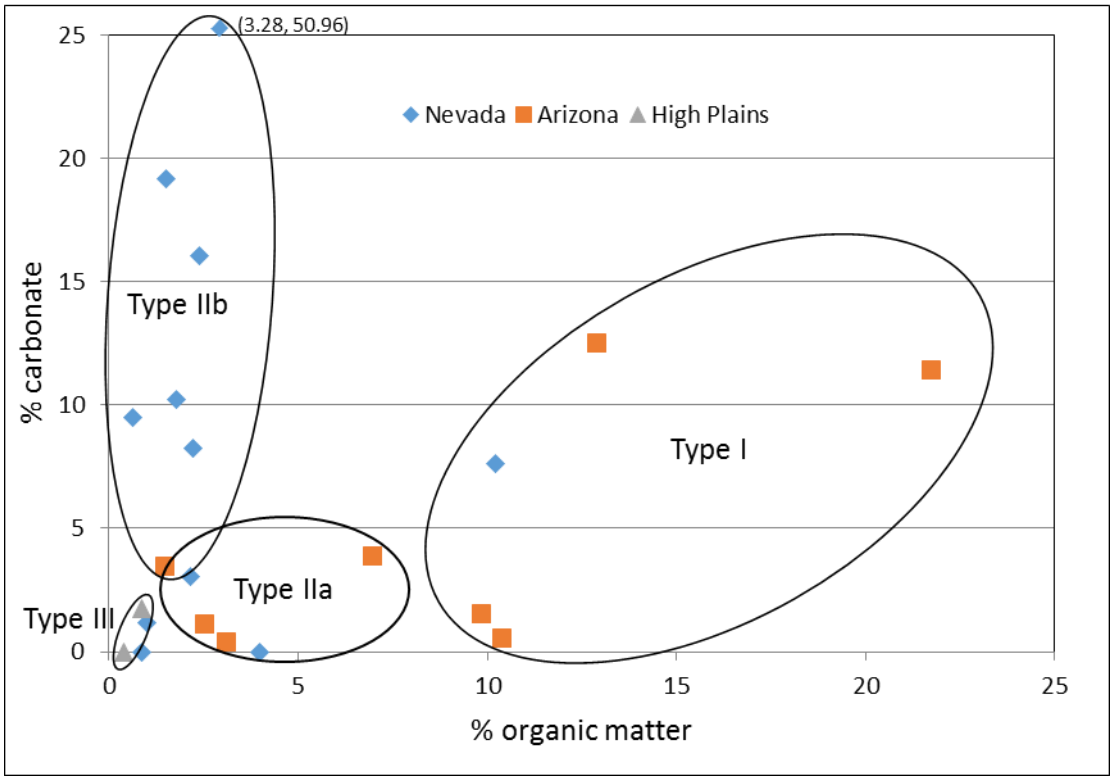

Figure 7. Percent calcium carbonate versus percent organic matter among types I-III black mats. The two samples from Nevada that plot near the type III black mats do not fit into a category based on their geochemical and micromorphological characteristics.

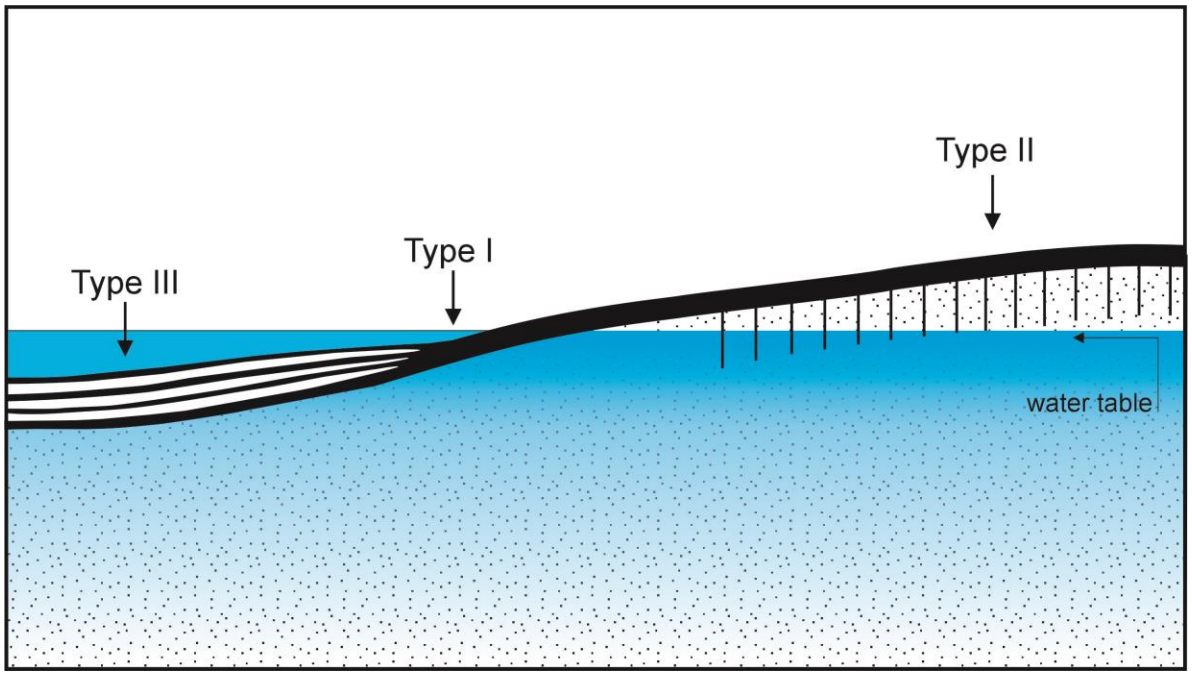

Figure 8. Facies model for black mat formation. The model demonstrates how the relationship between groundwater and topography can affect the morphological and chemical characteristics of black mats. Note that this exact progression is not seen in any region where black mats where sampled. Type III is geographically restricted to the High Planes while type I and II area seen grading into each other in both Arizona and Nevada.

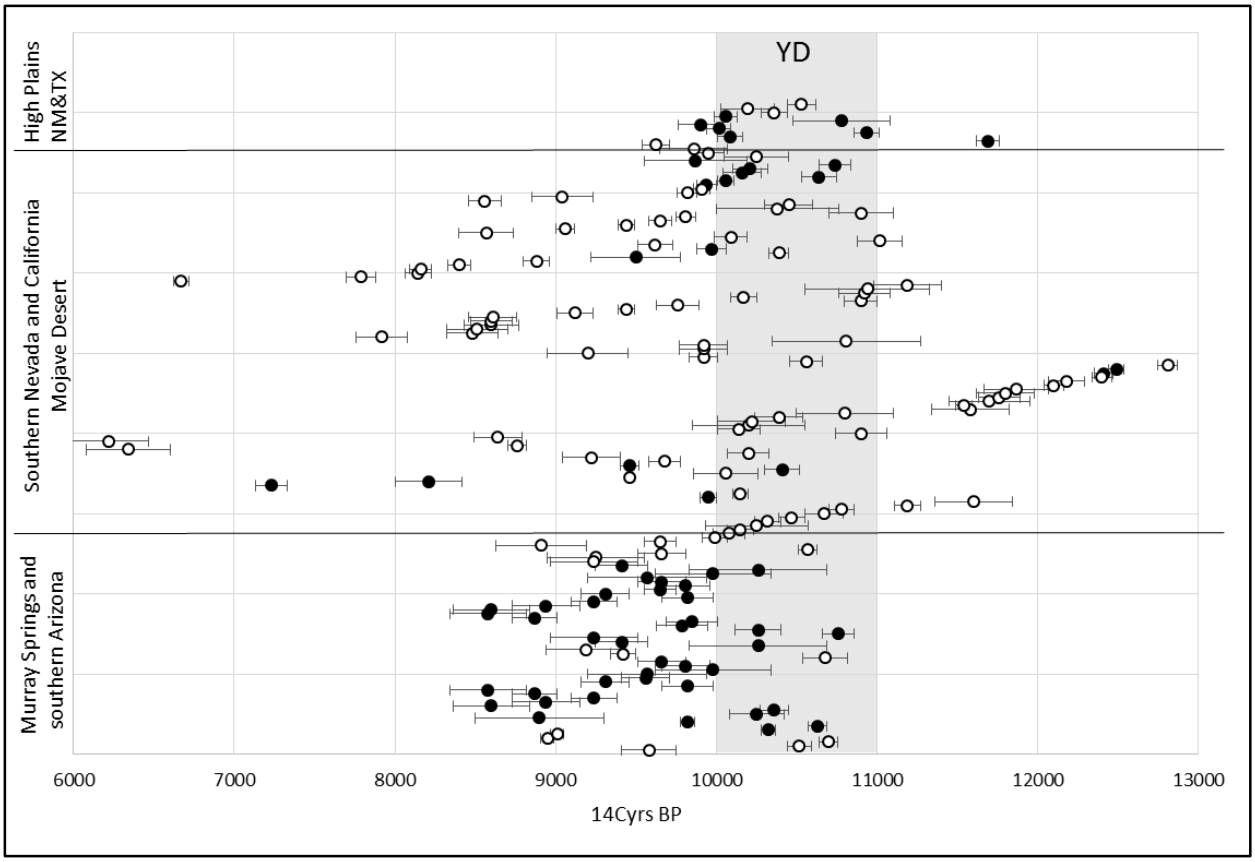

Figure 9. All radiocarbon dated black mat samples in the areas near the sampling locations. Filled circles indicate radiocarbon dates taken from the sample locality, and in most cases the ^{14}C sample was collected from the same outcrop as the micromorphology samples. Open circles indicate dates from nearby localities. Dating Sources: Haynes, 1967; Haas and Holliday, 1986; Quade, 1986; Haynes, 1995; Narvaez, 1995; Quade et al., 1995; Quade et al., 1998; Jull et al., 1999; Huckleberry et al., 2001; Haynes, 2007a; Haynes, 2008; Hatte et al., 2010; Pigati et al., 2011; Pigati et al., 2012.

Table 1
Descriptions of each black mat type with a photo of the characteristic mircromorphological features, a list of samples for each type, and their interpreted depositional environment.

Type	Representative Photo	Description	Samples	Paleoenvironmental interpretation
Type I	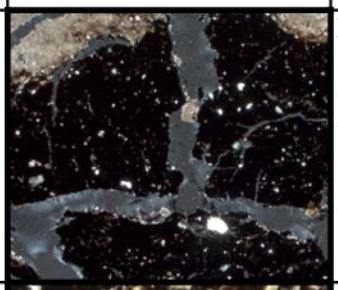	Massive to layered, blocky structure, composed of finely fragmented opaque organic matter, little mineral component, phytoliths abundant. Micromass is black and opaque.	MS13-1A&B, SP14-3, MS13-2A&B, BM1, MS14-4	Shallow standing water with periodic desiccation causing peat-like accumulation of organic matter.
Type IIa	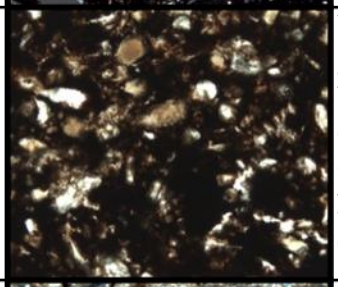	Vertic properties: slickenslides, grano, poro,cross,&mono striated b-fabrics, fine to coarse quartz component, massive to blocky. Groundmass darkly stained by humic acids. Coarse mineral component higher (9-49%).	BM3, BM2, SP 13-2A&B, svf87-9, BM1, MS14-4, SP13-1B BM6, SP14-4	Very productive moist soils, experienced wetting and drying. Highly bioturbated causing absence of layering and fragmented, well mixed organic matter.
Type IIb	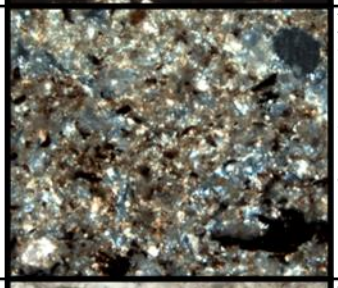	Higher carbonate content with lighter colored micromass, abundant iron impregnations, fragmented organic matter, gastropod shells.	CS81 carb 6, Cac Spr. Mol 31, Pah Carb 20, Pah Carb 26, BM6, SP14-4	Productive wet meadow soils that formed in a carbonate rich parent material, mixed through bioturbation.
Type III	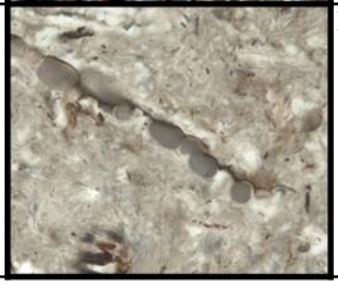	Laminated, fine grained, diatoms and phytoliths abundant.	LL13-1, CS14-1	Permanent standing water, lacustrine sediments, low energy environment.

Table 2
Basic geographic, geochemical and chronologic characteristics of the black mat samples.

	Sample name	Thin section ID	Location	% o.m.	%$CaCO_3$	Type	Age ^{14}Cyrs/relative	Dating source
Nevada	svf87-9	1	Sandy valley	4.0	0	IIa	9620±110	Quade et al. 1998
	Gilcrease1	2	Gilcrease Ranch	1.0	1.2	-	10560±100, 9920±90	Narvaez 1995
	CS81 carb 6	3	Corn Creek Flat	3.3	51.0	IIb	9220±180	Quade et al. 1995
	Pah Carb 20	4	Browns Springs	2.2	8.2	IIb	7230±100	Quade et al. 1998
	Cac.Spr. Mol 31	5	Cactus Springs	1.5	19.2	IIb	<9460±60	Quade et al. 1998
	Pah Carb 26	27	Stump Spring	2.1	3.1	IIb	10090±100	Quade et al. 1998
	Cac.Spr Carb 7[#]	-	Cactus Springs	0.9	0	-	10060±200	Quade et al. 1998
	Cac.Spr.Carb 6[#]	-	Cactus Springs	1.8	10.2	IIb	10410±110	Quade et al. 1995
	Gilcrease 16 [#]	-	Gilcrease Ranch	10.2	7.6	I	10560±100, 9920±90	Narvaez 1995
	Gilcrease 22[#]	-	Gilcrease Ranch	0.6	9.5	IIb	10560±100, 9920±90	Narvaez 1995
	CSC89-7[#]	-	Corn Creek Flat	2.4	16.1	IIb	10,200±130	Quade et al. 1998
Arizona	MS13-1A&B	7, 10	Murray Springs Area4	9.9	1.5	I	10760±100,10260±140	Haynes 2007a
	MS13-2A	13	Murray Springs Profile B	12.9	12.5	I	10325±45, 10630±60, 9820±45	Jull et al. 1999
	MS13-2B1&2	14,15	Murray Springs Profile B	21.7	11.4	I	10325±45, 10630±60, 9820±45	Jull et al. 1999
	MS14-4	23	Murray Springs TR 22	3.1	0.4	IIa	10260±430, 9410±160, 9240±270	Haynes 2007a
	SP13-1B	17^	San Pedro Valley	7.0	3.9	IIa	Directly overlies mammoth teeth	J. Ballenger
	SP13-2A&B	18, 19	San Pedro Valley	2.5	1.1	IIa	Directly overlies mammoth teeth	J. Ballenger
	SP14-3	24	San Pedro Valley	10.4	0.5	I	-	-
	SP14-4	26	San Pedro Valley	1.5	3.5	IIab	Overlies Pleistocene horse tooth	This study
	BM1[+]	BM1	San Pedro Valley	-	-	IIa	-	-
	BM2[+]	BM2	San Pedro Valley	-	-	I	-	-
	BM3[+]	BM3	San Pedro Valley	-	-	IIa	-	-
	BM6[+]	BM6	San Pedro Valley	-	-	IIab	Overlies Pleistocene horse bone	J. Ballenger
New Mexico	CS-14-1	20	Blackwater Draw	0.9	1.8	III	10740-9860	Haynes 1995
Texas	LL13-1	21,22	Lubbock Lake	0.4*	0*	III	10780-9905	Haas et al. 1986

*From Holliday 1985b, [+] thin sections from J. Ballenger [#]Bulk sediment sample only, no thin section, ^ poorly preserved thin section sample, no description included in Table 2.

Appendix

Table A1

Micromorphological descriptions of black mat thin sections. For an overview of the terminology used see Stoops (2003).

Sample ID	Coarse Fraction	Microstructure	Voids	c/f dist	Micromasss and b-fabric	Pedofeatures	Organic matter
SVF87-9	Very well sorted quartz grains (5%)	Weak subangular blocky	Channels, vughs, planes	Open porphyric	Calcitic speckled	Illuvial clay, iron staining and hypocoatings	Dark stains, large phytoclasts and phytoliths
Gilcrease 1	Well sorted silt sized quartz grains (37%), feldspar and mica rare	Granular	Complex packing, channel	Chitonic	Brown, weak granostriated		Polymorphic o.m.*
CS81Carb 6	Silt sized quartz grains rare (<1%)	Granular to subangular blocky	Compound packing, channels, vughs, planes	Fine monic	Calcitic,(dull tan), very weakly speckled	Transported micrite grains, rounded	Lath shaped phytoclasts dispersed through matrix
Pah Carb20	Well sorted silt sized quartz grains (6%), mica rare	Strong subangular blocky	Channels and intrapedal planes	Open porphyric	Micrite with visible crystals. Tan to brown with patchy o.m. stains	Iron impregnations and hypocoatings,	Large phytoclasts with visible structure, fragmented gastropod shells
Calc Spr Mol31	Well sorted silt sized quartz grains (10%), mica rare	Granular to massive with channels	Complex packing, channel	Single to fine equal enaulic	Inhomogeneous, calcitic,	Rounded, transported, micrite grains	Gastropod shells, small phytoclasts, also stains
Pahcarb26	Very well sorted silt sized quartz (9%)	Massive/channel	Channel and cracks	Open porphyric	Inhomogeneous, calcitic, brown-tan, weak speckled	Rounded calcite clasts, Iron impregnations	Large phytoclasts, rare fragmented shell
MS13-1A	Very well sorted, silt and fine sand quartz (4%)	Angular blocky	Channels, intrapedal planes	Open porphyric	Opaque black, very weak speckled	Needle calcite in voids, mite feces, iron impregnations	Opaque phytoclasts, phytoliths:~1%
MS13-1B	Very well sorted, silt and fine sand quartz (5%)	Angular blocky	Channels, intrapedal planes	Open porphyric	Opaque black, very weak speckled	Needle calcite in voids, mite feces	Opaque phytoclasts, phytoliths
MS13-2B1	Well sorted silt to fine sand sized quartz grains (8%).	Massive layered, channel	Channel, planes	Open porphyric	Layered, black organic rich and tan, micrite	Root channels	Fragmented shells, bone, opaque phytoclasts

MS13-2B2	Moderately sorted silt to medium sand sized quartz grains (2-7%) varies in different layers.	Sub-angular blocky to massive layered	Channel, intrapedal planes	Open porphyric	Layered, black organic rich and tan, micrite	Root channels with needle calcite	Fragmented shells, bone, opaque phytoclasts
MS14-4	Very poorly sorted rounded to subrounded, gravel to medium sand sized quartz grains (49%)	Crumb	Complex packing	Double spaced equal enaulic	Dark brown-brown , grano and parallel striated, speckled in layered area	Modern root and mite feces	Phytoliths rare, stains
SP13-1B	Poorly sorted, rounded, fine gravel to silt sized quartz grains (32%), feldspar (2%)	Massive with channels	Channel, vughs	Open porphyric	Patchy dark brown to grey, weak poro, grano and crossstriated		Phytoliths: 2-5%, polymorphic o.m., dark stains
SP13-2A	Poorly sorted subrounded coarse sand to silt sized quartz grains (19%) feldspar (1%)	Subangular blocky	Planes, cracks, some channels	Double spaced porphyric	Brown, weak speckled, some mono and porostriated		Phytoliths rare, small phytoclasts
SP13-2B	Moderately sorted, fine gravel to silt sized rounded quartz grains (14%), mica (1%)	Subangular blocky to angular blocky	Planes, cracks, complex packing	Double to open porphyric	Brown-light brown, grano, poro and crossstriated and speckled	Iron staining, root bioturbation	Phytoliths rare, small phytoclasts
SP14-3	Poor- moderately sorted, medium sand to silt sized particles, abundance increases (6-11%)upwards, graded bedding	Highly separated subangular blocky, some massive	Planar, vughs, channels	Double spaced porphyric	Brown to black, Weakly speckled	bioturbation	Phytoliths:2%, opaque phytoclasts, polymorphic o.m.
SP14-4	Well sorted, fine sand to silt sized quartz grains (11%), mica grains rare	Well-developed subangular blocky to columnar	Planar, channels	Double spaced porphyric	Light-brown grano, poro, crossstriated, and weak speckled	Iron stains, burrows and mite feces	Phytoclasts, polymorphic o.m.
BM1	Poor-moderate sorted coarse sand to silt sized quartz grains (35%), feldspar and mica rare	Intergrain microaggregate to subangular blocky	Complex packing, channels	Chitonic and single to double fine enaulic	Dark brown-black o.m. aggregates	Thick Needle calcite, clay clasts	Phytoliths:2%, polymorphic o.m.

BM2	Poorly sorted very coarse sand to silt sized quartz grains (32%), mica and feldspar rare	Massive with cracks	Channels, cracks (slickensides)	Double spaced porphyric	Light-Dark brown, o.m. stains. Strong monostriated and speckled, some grano/porostriated	Clay clasts	Phytoliths .5%, polymorphic o.m., large phytoclasts with cell structure rare
BM3	Well sorted, dominantly silt sized with medium and fine sand sized quartz grains (13%)	Well-developed subangular blocky with highly separated peds	Planes, cracks	Double spaced porphyric	Homogeneous dark brown, weak speckled	Clay clasts, iron staining	Phytoliths 1%, large phytoclasts with cell structure and polymorphic o.m. rare
BM6	Very well sorted fine sand to silt sized quartz grains (9%), rounded micrite fragments rare	Well developed-moderate angular blocky, moderate to well separated	Cracks (slickensides), planes channels,	Double spaced porphyric	Brown-light brown, Strong mono, grano, crossstriated and speckled	Micrite clasts, iron staining	phytoclasts
CS-14-1	Well sorted fine sand to silt sized quartz grains (13%), some layering	Massive with channels	Channels	Massive layered	Light grey to tan, very weak speckled, monostriated rare	Root channels	Phytoliths, diatoms, phytoclasts all abundant
LL13-1	Silt sized quartz grains (3%), distinct layering	Massive with channels	Channels, complex packing	Massive layered	Light grey, weak speckled	Root channels, Phosphate staining	Phytoliths, diatoms, phytoclasts all abundant

*organic matter

Appendix

Table A2
Black mat radiocarbon dates used in Fig. 9.

Location	Site/ Unit Name	Sample ID	^{14}C age	Source
Arizona	Chapo Ranch, AZ	AA-53781	9580±170	Haynes 2008
	Chapo Ranch	AA-52885	10516±75	Haynes 2008
	Chapo Ranch	AA-52886	10696±57	Haynes 2008
	Horsethief Draw, Earp Marl	SPV02-HD1-7	8950±40	Pigati et al. 2009
	Horsethief Draw, Earp Marl	SPV07-HD1-7	9010±40	Pigati et al. 2009
	Murray Springs, Profile B	AA-26211	10325±45	Jull et al. 1999
	Murray Springs, Profile B	AA-26212	10630±60	Jull et al. 1999
	Murray Springs, Profile B	AA-26210	9820±45	Jull et al. 1999
	Murray Springs, Area 1	16MS67A	8900±400	Haynes 2007a
	Murray Springs, Area 1	17ms67c	10250±170	Haynes 2007a
	Murray Springs, Area 1	15ms67b	10360±90	Haynes 2007a
	Murray Springs, Trench 13N	51A70	8600±240	Haynes 2007a
	Murray Springs, Trench 13N	51A70	8940±210	Haynes 2007a
	Murray Springs, Trench 13N	51A70	9240±140	Haynes 2007a
	Murray Springs, Trench 13N	52A70	8870±140	Haynes 2007a
	Murray Springs, Trench 13N	52A70	8580±240	Haynes 2007a
	Murray Springs, Trench 13N	50A70	9820±160	Haynes 2007a
	Murray Springs, Trench 13N	49A70	9310±150	Haynes 2007a
	Murray Springs, Trench 13N	48A70	9560±150	Haynes 2007a
	Murray Springs, Trench 13N	44A70	9570±370	Haynes 2007a
	Murray Springs, Trench 13N	44A70	9980±360	Haynes 2007a
	Murray Springs, Trench 13N	47A70	9810±150	Haynes 2007a
	Murray Springs, Trench 13N	46A70	9660±150	Haynes 2007a
	Murray Springs, North of RR	2A70	10680±140	Haynes 2007a
	Murray Springs, North of RR	2A70	9420±80	Haynes 2007a
	Murray Springs, North of RR	2A70	9190±250	Haynes 2007a
	Murray Springs, Area 8	28A70	10260±430	Haynes 2007a
	Murray Springs, Area 8	28A70	9410±160	Haynes 2007a
	Murray Springs, Area 8	28A70	9240±270	Haynes 2007a
	Murray Springs, Area 4	H-7	10760±100	Haynes 2007a
	Murray Springs, Area 4	4 29	10260±140	Haynes 2007a
	Murray Springs, Trench 28	23-21	9790±160	Haynes 2007a
	Murray Springs, Trench 28	23-21	9850±160	Haynes 2007a
	Murray Springs, Trench 13N	52	8870±140	Haynes 2007a
	Murray Springs, Trench 13N	52	8580±240	Haynes 2007a
	Murray Springs, Trench 13N	51	8600±240	Haynes 2007a
	Murray Springs, Trench 13N	51	8940±210	Haynes 2007a
	Murray Springs, Trench 13N	51	9240±140	Haynes 2007a

	Murray Springs, Trench 13N	50	9820±160	Haynes 2007a
	Murray Springs, Trench 13N	49	9310±150	Haynes 2007a
	Murray Springs, Trench 13N	48	9650±100	Haynes 2007a
	Murray Springs, Trench 13N	47	9810±150	Haynes 2007a
	Murray Springs, Trench 13N	46	9660±150	Haynes 2007a
	Murray Springs, Trench 13N	44	9570±370	Haynes 2007a
	Murray Springs, Trench 13N	44	9980±360	Haynes 2007a
	Murray Springs, Trench 18	28	10260±430	Haynes 2007a
	Murray Springs, Trench 18	28	9410±160	Haynes 2007a
	Murray Springs, Trench 18	28	9240±270	Haynes 2007a
	Naco site AZ	3a	9250±30	Haynes 2008
	Red Peak Valley, AZ	4a	9660±150	Haynes 2008
	Seff Locality, Earp Marl	SPV05-SL-1	10570± 60	Pigati et al. 2009
	Wilcox Playa AZ	Stratum C	8910±280	Haynes 2008
California	Valley Wells, Unit E2b	VW7-19	9650±100	Pigati et al. 2011
	Valley Wells, Unit E2b	VW2-7	9990±80	Pigati et al. 2011
	Valley Wells, Unit E2b	VW1-3	10080±100	Pigati et al. 2011
	Valley Wells, Unit E2b	VW26-69	10150±80	Pigati et al. 2011
	Valley Wells, Unit E2b	VWF87-1b	10250±320	Quade et al. 1995
	Valley Wells, Unit E2b	VW23-67	10320±80	Pigati et al. 2011
	Valley Wells, Unit E2b	VW23-67	10470±80	Pigati et al. 2011
	Valley Wells, Unit E2b	VW1-3	10670±120	Pigati et al. 2011
	Valley Wells, Unit E2b	VW7-19	10780±80	Pigati et al. 2011
	Valley Wells, Unit E2b	VW24-68	11190±240	Pigati et al. 2011
	Valley Wells, Unit E2b	VWC87-3b	11600±240	Quade et al. 1998
	Dove Spring	MOJ07-105-DS	9950±50	Pigati et al. 2012
	Dove Spring	MOJ07-104-DS	10150±50	Pigati et al. 2012
	Dove Spring	MOJ07-109-DS	10510±60	Pigati et al. 2012
Nevada	Browns Springs	PVcarb22b	7230±100	Quade et al. 1998
	Browns Springs	PVCarb.21b	8210±210	Quade et al. 1998
	Cactus Springs	Cac.Spr.Mol 31	<9460±60	Quade 1989
	Cactus Springs	Cac.Spr.Carb 7	10,060±200	Quade et al. 1998
	Cactus Springs	Cac.spr.Carb 6	10,410±110	Quade et al. 1995
	Cactus Springs	Cac SprCarb-2b	9460±60	Quade and Pratt 1989
	Cactus Springs	Cac SprCarb-2b	9680±100	Quade and Pratt 1989
	Corn Creek Flat	CS81 Carb 6	9220±180	Quade et al. 1995
	Corn Creek Flat	CSC87-7	10200±130	Quade et al. 1998
	Corn Creek Flat	CSC87-5b	6340±260	Quade et al. 1998
	Corn Creek Flat	CSC87-9b	8760±60	Quade et al. 1998
	Corn Creek Flat	CSCarb.-11a	6220±250	Quade 1986
	Corn Creek Flat	CS81Carb11b	8640±150	Quade 1986
	Corn Creek Flat	CS81 carb. 3a	10090±160	Quade 1986
	Corn Creek Flat	CS81carb.3b	10140±130	Quade et al. 1995

Corn Creek Flat	75a	10200±350	Haynes 1967
Corn Creek Flat	CS81Carb 13b	10220±210	Quade et al. 1998
Corn Creek Flat	CSC87-6b	10390±150	Quade et al. 1998
Corn Creek Flat	76a	10800±300	Haynes 1967
Corn Creek Flat	CSC87-2b	11580±240	Quade et al. 1998
Corn Creek Flat	CSWood1	11540±50	Quade et al. 1998
Corn Creek Flat	77a	11700±250	Haynes 1967
Corn Creek Flat	CSC87-1b	11760±130	Quade et al. 1995
Corn Creek Flat	CSC87-3b	11800±180	Quade et al. 1998
Corn Creek Flat	CSC87-8b	11870±200	Quade et al. 1998
Corn Creek Flat	CSC27b	12100±60	Quade et al. 1998
Corn Creek Flat	CSCarb.30b	12180±110	Quade et al. 1998
Corn Creek Flat	CSCarb.27b	12400±60	Quade et al. 1998
Corn Creek Flat	CSCarb.28a	12410±60	Quade et al. 1998
Corn Creek Flat	CSCarb.28b	12490±50	Quade et al. 1998
Corn Creek Flat	CSC-29b	12810±60	Quade et al. 1998
Gilcrease Ranch, Unit II	Beta-78244	10560±100	De Narvaez 1995
Gilcrease Ranch, Unit II	Beta-78243	9920±90	De Narvaez 1995
Gilcrease Ranch	62a	9200±250	Haynes 1967
Gilcrease Ranch	63a	9920±150	Haynes 1967
Gilcrease Ranch	19b	10810±460	Haynes 2008
Hidden Valley	PVCarb.-47b	7920±160	Quade et al. 1998
Hidden Valley	PVCarb.37b	8480±160	Quade et al. 1998
Hidden Valley	PVCarb.-10b	8510±190	Quade et al. 1998
Hidden Valley	PVCarb.-34b	8600±170	Quade et al. 1998
Hidden Valley	PVCarb-41b	8600±130	Quade et al. 1998
Hidden Valley	PVCarb.-29b	8610±150	Quade et al. 1998
Hidden Valley	PVCarb.-36b	9120±110	Quade et al. 1998
Hidden Valley	PVCarb-27b	9440±50	Quade et al. 1998
Hidden Valley	PVCarb-38b	9760±130	Quade et al. 1998
Hidden Valley	PVCarb-26b	10090±100	Quade et al. 1998
Hidden Valley	PVCarb-36b	10170±80	Quade et al. 1998
Hidden Valley	PVCarb-39b	10920±160	Quade et al. 1998
Hidden Valley	PVCarb-33b	10940±390	Quade et al. 1995
Hidden Valley	PVCarb-31b	11190±210	Quade et al. 1995
N. Coyote Springs	NCySC-4b	6670±50	Quade et al. 1998
N. Coyote Springs	NCySC-6b	7790±90	Quade et al. 1998
N. Coyote Springs	NCySC-8b	8145±80	Quade et al. 1998
N. Coyote Springs	NCySC-3b	81600±70	Quade et al. 1998
N. Coyote Springs	NCySC-9b	8400±70	Quade et al. 1998
N. Coyote Springs	NCySC-7b	8880±80	Quade et al. 1998
N. Coyote Springs	NCySC-5b	9500±280	Quade et al. 1995
N. Coyote Springs	NCySC-2b	10390±60	Quade et al. 1998

	S. Coyote Springs	SCySCarb-1b	9970±90	Quade et al. 1995
	Sandy valley	SVF87-9	9620±110	Quade et al. 1998
	Sandy Valley	SAVCarb-1b	11020±140	Quade et al. 1995
	Stump Spring	Pah Carb 26	10090±100	Quade et al. 1998
	Stump Spring	Pvcarb.-15a	8570±170	Quade et al. 1995
	Stump Spring	PVCarb.-14b	9060±60	Quade et al. 1998
	Stump Spring	PVCarb.-27b	9440±50	Quade et al. 1998
	Stump Spring	PVCarb-13b	9650±70	Quade et al. 1998
	Stump Spring	PVCarb-12b	9810±60	Quade et al. 1998
	Stump Spring	PVCarb-7b	10090±200	Quade et al. 1998
	Stump Spring	PVCarb-11b	10380±380	Quade et al. 1995
	Stump Spring	PVCarb-8a	10450±150	Quade et al. 1998
	Sunshine locality NV	69781	8560±100	Huckleberry et al. 2001
	Sunshine locality NV	86200	9040±190	Huckleberry et al. 2001
	Sunshine locality NV	69782	9820±60	Huckleberry et al. 2001
	Sunshine locality NV	86202	9910±50	Huckleberry et al. 2001
	Sunshine locality NV	86203	9940±60	Huckleberry et al. 2001
	Sunshine locality NV	86204	10060±50	Huckleberry et al. 2001
New Mexico	Blackwater Draw	AA-1361	10640±110	Haynes 1995
	Blackwater Draw	AA-1363	10160±120	Haynes 1995
	Blackwater Draw	AA-1364	10210±110	Haynes 1995
	Blackwater Draw	AA-1362	10740±100	Haynes 1995
	Blackwater Draw	A-4702	9870±320	Haynes 1995
	Blackwater Draw	A-1372	10250±200	Haynes 1995
	Blackwater Draw	AA-2261	9950±100	Haynes 1995
	Blackwater Draw	AA-1412	9860±210	Haynes 1995
	Pounds Playa NM	AA-66775L	9620±90	Haynes 2008
	Pounds Playa NM	AA-66775H	11700±70	Haynes 2008
Texas	Aubrey site, TX,	Strata E&G	10085±80	Haynes 2008
	Aubrey site, TX	Strata E&G	10940±80	Haynes 2008
	Lubbock Lake	SI-3203	10015±75	Haas and Holliday 1986
	Lubbock Lake	SI-4975	9905±140	Haas and Holliday 1986
	Lubbock Lake	LL65-2A	10780±300	Hatte et al. 2010
	Lubbock Lake	SMU-251	10060±70	Haas and Holliday 1986
	Lubbock Lake	SI-3200	10360±80	Haas and Holliday 1986
	Lubbock Lake	SI-4976	10195±165	Haas and Holliday 1986
	Lubbock Lake	SMU-285	10530±90	Haas and Holliday 1986